CHALMERS

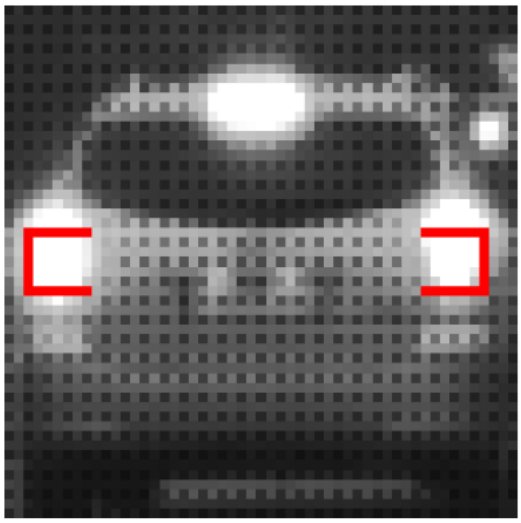

Active Safety Sensor Verification

Development of Image Analysis Support Tool

Master's Thesis

JOACHIM RUKIN PERSSON

Department of Signals & Systems
Chalmers University of Technology
Gothenburg, Sweden 2012
Master's Thesis EX041/2012

Active Safety Sensor Verification
Development of Image Analysis Support Tool

Master's Thesis EX041/2012

Department of Signals & Systems
Chalmers University of Technology
SE-41296 Göteborg
Sweden

Tel. +46-(0)31 772 1000

Department of Signals & Systems
Göteborg, Sweden 2012

Active Safety Sensor Verification
Development of Image Analysis Support Tool
Master's Thesis
JOACHIM RUKIN PERSSON
Department of Signals & Systems
Chalmers University of Technology

Abstract

Active safety sensing systems monitor the environment in order to evaluate traffic situations and to assess the risk of a collision or an accident. In order to do so, these systems rely on the output from sensors such as radars and cameras. The sensor systems have to fulfill requirements to assure the functionality of the active safety system and therefor it is important to verify the output of these sensors. The output is verified using logged data (CAN, video, etc.) gathered by test vehicles in real traffic. The number of false, missed and true detections is a measure of the performance of the sensor system. True and false detections are evaluated by analyzing the output of the sensor system, whereas missed detections demand more attention since there is no information about when or where they occurred. The goal of this thesis is to improve the quality and efficiency of sensor system verification and the main focus will be on brake light detection. A stand-alone vision based brake light detection algorithm is developed to automatically find brake light events. In addition to that a support tool is designed to make the evaluation of the brake light events quick and easy.
The suggested brake light detection algorithm has a false detection rate of 15%, but misses only 1% of all true brake light events. For verification purposes it is preferred to optimize against high true positive detection over low false positive ratio.
The automatic brake light detection together with the evaluation support tool makes it possible to decrease the time needed for verification of the sensor system's brake light detection by almost 90%.

Keywords: Sensor Verification, Brake Light Detection, Computer Vision, Image Analysis, Pattern Recognition, Tracking

Acknowledgements

I have had the good fortune to receive advice and guidance from *Anders Sandberg*, my supervisor at *Delphi - Electronics & Safety*. I would also like to express my gratitude towards *Artur Chodorowski*, who has been supportive and showed interest in my thesis project. My thanks and appreciations also go to my colleagues and friends for all valuable discussions.

Joachim Rukin Persson
Gothenburg, 20 May 2012

Contents

List of Figures

List of Tables

1

Introduction

Active safety systems are automotive functions, which purpose is to make the traffic safer, by reducing the risk for accidents. These functions are continuously evaluating the traffic environment with the use of sensors like radars and cameras. Algorithms then use the sensor outputs to decide when the active safety system is to be activated in order to either warn the driver or to mitigate and try to avoid a collision or accident automatically. Examples of such systems are Lane Departure Warning, Volvo's City Safety, CMbB (Collision Mitigation by Braking). Active safety systems are thus a combination of the sensor system (radar and camera) and algorithms for threat assessment and decision-making to provide increased safety for the road-users. The output from the radar in the sensor system can be position, range and range-rate of other objects (vehicles) and the vision system can provide object recognition (pedestrians) and detection of lane markers. The vision system has the possibility to provide more detailed information about the surroundings and the detected objects regarding specific features, e.g. various traffic signs and lane markers, something that the radar is incapable of. Brake lights on vehicles in adjacent lanes is another object feature that can be part of the threat assessment, can't be detected by the radar.

1.1 Background

Traffic situations are often very complex and mitigating active safety systems like for instance the auto-brake function must not jeopardize the safety of any road-user at any time. The performance of an active safety system can be evaluated based on its decision-making performance, that is, the error-rate for given and not given warnings (or actions). A system that gives false warnings (false positives), misses warnings (false negatives) or nuisance alerts will affect the driver's adaptation to the system, which will more likely end with deactivation of the given system. So, one can say that the development of active safety systems is not an easy task. One have to consider not only the technical

issues but one also has to take the behavioral aspects of how persons drive and act in different traffic situations into account. To make an active safety system ready for production, i.e. to be installed in vehicles, both the sensor system performance and the complete active safety system performance have to be validated. The requirements for the sensor system have to be fulfilled to ensure that the algorithms in the active safety system will provide all information needed in order to make the right decisions. An example to give a better understanding of what the requirements are: "The sensor system have to detect visual lane markers in at least 99% of all cases regardless of light- and weather conditions". The functionality of the sensor system therefor has to be tested and evaluated in various traffic scenarios, different light- and weather conditions and so on, for the the sensor system provider to ensure that the sensor system performs according to the requirements. Simulations and bench-testing can be used in the early stages of the development but the final testing of the performance has to be made by installing the sensor system in actual cars equipped with logging equipment to store CAN-data and sensor data (video and radar data). This data is also used to analyze and solve problem scenarios in which the sensor system fails to perform as aspected.

1.2 Problem definition

In the verification process of the sensor system used in active safety systems one has evaluate the output of the sensor system which can be summarized in Table 1.1. *True Positives* (correct detections) are fairly easy to check, one just have to go through the data in which the sensor system has an output and doing so will in turn give you the number of *True Positives* or *False Positives* (false detections). *True Negatives* are not necessary to assess. But the *False Negatives* (missed detections) have to evaluate all data since no indication of where to look is available. This so called *ground truthing* is obviously a time consuming and monotonous task to do manually, especially since the OEMs require verification of all the essential sensor system outputs on a large data set.

Table 1.1: Sensing system output

	Event	No Event
Output	True Positives	False Positives
No Output	False Negatives	True Negatives

1.3 Purpose and objective

The purpose of this Master's thesis project is to improve the performance and the efficiency of active safety sensor verification. A vision-based brake light detection algorithm will be developed to find brake light events regardless of vehicle speed, range (distance

to object), lamp type (LED or non-LED), and traffic environment in order to minimize the need for manual ground truthing.
The main task is to develop an image analysis script in MATLAB to analyze logged video data from real traffic situations and to detect and classify lit brake lights on vehicles in field of view. The task is divided into three subtasks:

- Rear light analysis.
- Extract regions of interest (ROI) from image frames, algorithm development for bright-spot detection and extraction of their properties and algorithm development for classification of brake lights.
- Design a support tool for evaluation of true, missed, and false events from the sensor system.

1.4 Constraints

The project has the following constraints:

- Motorcycles are excluded.
- No brake light detection in daytime.
- The vehicle must have a center brake light.

2

Related Work

This Chapter contains the study of various possible methods or approaches of how to detect brake-lights or how to solve similar tasks.

Several papers on vision-based vehicle- and/or brake-light detection suggest methods using various types of image pre-processing to extract features of bright spots such as area, intensity, shape, angle, position and so on. The image pre-processing is a kind of image manipulation to enhance desired features and to filter out undesired features or artifacts that possibly could effect the performance in the following analysis stage negatively [1–9]. Feature extraction and selection are often done by the use of statistics of for instance brake-light position relative to each other and relative to ground [1]. Other assumption such as brake-light symmetry and predefined regions of interest (ROI) have shown to be helpful in the pre-classification process [5, 6, 8, 9]. When it comes to the classification and object recognition some papers describes methods based on supervised machine learning and artificial intelligence techniques (AdaBoost or Support Vector Machine) [2, 4] where training samples are needed for the learning process. Discriminant analysis is a method often used in pattern recognition and machine learning. It is a way of distinguish two or more classes by finding a combination of their features [10]. The authors of [11] describes an alternative method to identify brake-lights on vehicles by using fast Fourier transform (FFT) of a pre-processed image frame and compare it with the FFT of the previous frame. A change in the image intensity can be detected in the frequency domain as a larger (brake-light activation) or smaller (brake-light deactivation) peak. Papers on vehicle detection often use Kalman filter tracking to estimate and track the position of objects [5, 6].

3

Analysis of Rear Lights

As mentioned in the introductory chapter, the functionality of the sensor system has to be evaluated before the active safety system can be put into production and be sold to the general public. The functional testing is performed in various scenarios and it's availability, i.e. the true detection rate, has to fulfill the requirements set by the OEMs. By logging sensor system output together with the vehicle's CAN-bus data, one can evaluate the performance of the sensor system and provide evidence of it's availability to the customers (OEMs). This chapter contains a brief presentation of the available data on which the following rear light analysis is based on.

3.1 Provided data

The provided materials are logged (vision, radar and CAN) data. This information is gathered in test-vehicles equipped with the sensor system together with equipment for logging and storing of the data just mentioned, although the focus in this project will be on the vision data.
The vision data is obtained via a vision system (vision sensor with vision algorithms for detection and classification of objects etc.), which is used together with a radar. This radar- and vision fused sensor system for active safety systems can be used for Forward Collision Warning (FCW) and Lane Departure Warning (LDW).

3.1.1 Vision output

Vision algorithms in the vision system detect and classify objects, such as vehicles and pedestrians, along with details about relative position, range-rate and geometrical features (width and height). Additionally, camera-based sensor systems can also provide more extrinsic features and properties describing the objects. The vision system can track several objects at a time, and each of these classified objects is assigned a so

called *bounding box*, which is a virtual frame that encloses the object and it is used for illustrating the tracking of the objects.

3.1.2 Video data

In addition to the vision output data on the CAN-bus, the video data itself is stored on a hard drive together with the saved CAN-bus data. This video data can be seen as the raw data of the vision system and it is used in this project to verify the vision system output. The vision system provides two videos, one with ”normal” exposure time and another with shorter exposure time. The second video is preferable to use for brake light detection due to the short exposure time, which in advance leads to a pre-thresholding so that only the really bright light sources are left in the image. In Figures 3.1 and 3.2 one image frame from two different video streams are shown, the left images are from the video stream using normal exposure time and the right images thus representing the video stream with short exposure time.

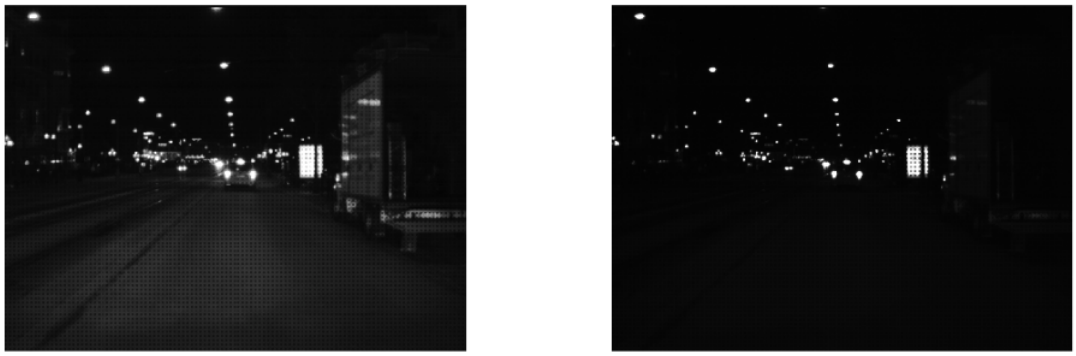

Figure 3.1: Image exposure time comparison 1.

As one can see, the images to the right (short exposure time) already look thresholded and many of the bright spots and bright areas that can be seen in the left images have disappeared or are of smaller size and less intensive in their brightness in the right images.

Figure 3.2: Image exposure time comparison 2.

3.2 Rear lights

In order to be able to detect rear- and brake lights of a car, one first has to know what to look for and where to look for it. This section is to give an overview of how these lights look like and where to find them. This project is not about finding and classifying vehicles, relevant vehicles are presumed already to have been detected and classified by the vision system and therefor these vehicles have been given a bounding box, which is the region of interest for the brake light detection. The purpose of this section is to present assumptions about the rear lights, that will be used in the vision algorithm further on. To avoid confusion further on, the term ”rear light” can be used for both brake lights and ordinary rear light i.e. no brake lights until the classification is done.

3.2.1 Side mounted rear lights

Obviously rear lights have the same shape and they appear in pairs, one on each side of the vehicle. The shape and position can vary a lot depending on the car model. In the bounding box the side rear lights are to be found somewhere in the area up to about one third of the width from each side. One third of the width might seem to be a lot, but the precision of the bounding box is not perfect and the vehicle is often moving around within it as well.

First assumption: *Side rear lights are located on the same height and in the area on each side in the bounding box, but at most about one third of the image width into the center of the image.*

The rear lights are symmetric and have the same size, brightness and shape. Although the shape of the rear lights is only possible to distinguish at close range, at longer distances the lights become all blurry which makes it hard to differentiate the shape of the lights.

Second assumption: *Side rear lights have the same size and brightness.*

3.2.2 Center high mounted stop lamps

Center high mounted stop lamps (CHMSL) are, as the name suggests, brake lights located high up, often in the rear window centered between the two side rear lights. CHMSL has been standard on all new cars in the US since the middle 1980's and in Europe since the end of the 1990's [12].

Third assumption: *All cars have a center high mounted stop lamp and it is located above or at the same level as the rear side lights.*

Just like for the side rear lights, the size and shape of the CHMSL is varying a lot from car to car which makes it difficult to make a general assumption about it's visual appearance. On the other hand a comparison of the size and intensity of the CHMSL to the size and intensity of the side rear lights, can be used to sort out false CHMSL:s (unknown light sources located at a position similar to a CHMSL). Here the size comparison is a rather "soft" measure, and basically it is used to sort out the extreme cases, i.e. very small CHMSL and large side rear lights or vice versa.

Fourth assumption: *Side rear lights and center high mounted stop lamps have similar brightness and the size difference between the CHMSL and the side brake lights is not too large.*

Another observation is that the shape of the center high mounted stop lamp varies from circular to elongated, tall and narrow CHMSL are however rare.

Fifth assumption: *Center high mounted stop lamps can have any shape but tall and narrow.*

3.2.3 Rear light characteristics

The brightness of the rear lights is more or less always totally saturated, meaning that the intensity is at it's maximum level. The main difference between rear lights and brake lights can be seen at the halos, hence the increase size for the rear light. For the side rear lights, the size difference between the non-braking and braking is not a trustworthy measure, especially since many cars have multiple rear-lights, out of which some lights are only lit when braking. This could lead to up to a doubling of the size of the side rear lights, while for other cars without multiple side rear lights, the change might be as low as 12.5% (which corresponds to a gain of 2.5 pixels for a rear light of 20 pixels). The images in Figure 3.3 illustrate the difference between rear lights and brake lights. In this case, there is a noticeable difference in the size difference for the side rear lights

but not for the change in intensity. (The red markers are only to visualize the rear light tracking and have nothing to do the with the feature extraction).

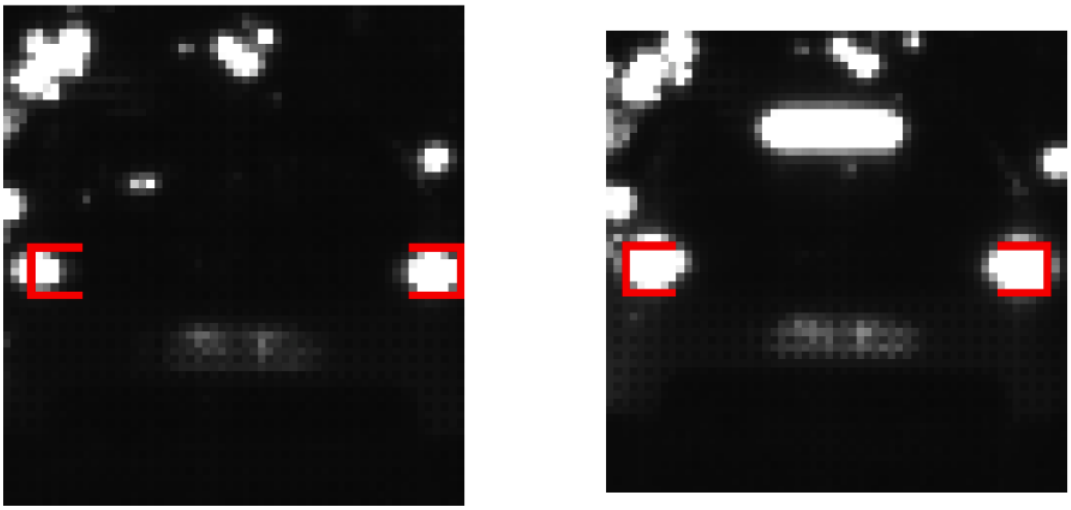

Figure 3.3: Rear lights (left image) and brake lights (right image) comparison.

4

Methodology

In this chapter the methodology is presented and the flow chart of the complete brake light detection algorithm is shown in Figure 4.1. This algorithm forms the basis for the rest of this chapter, which is divided into four sections: Processing, Analysis, Tracking and Classification, each of which contains a detailed description of its specific procedure.

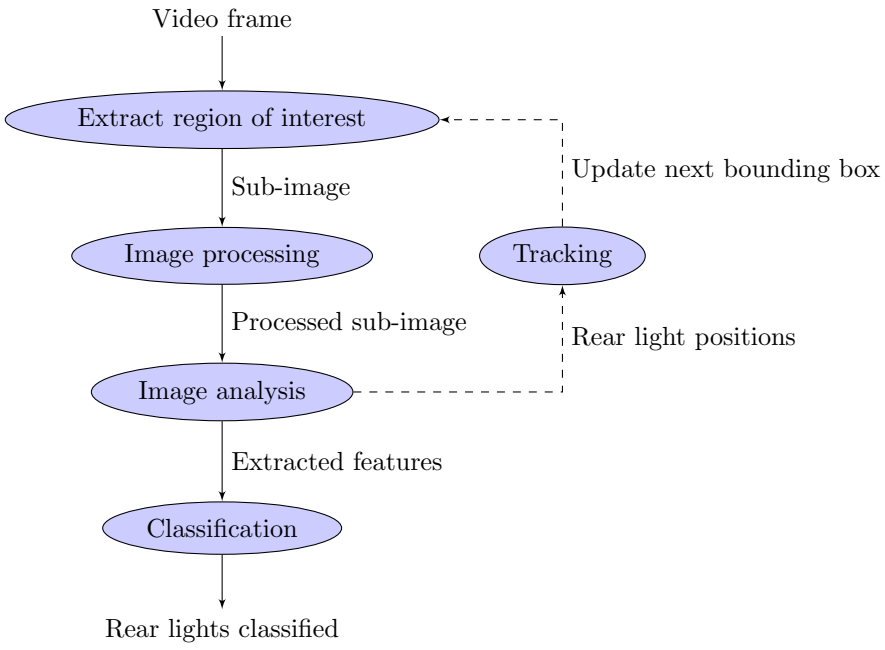

Figure 4.1: Brake light detection algorithm

4.1 Regions of interest extraction

The vision system provides several outputs, one of which is the image coordinates for the bounding box that encloses the detected and classified objects in the field of view (FOV). These coordinates are used to extract the regions of interest (ROI), hence the vehicle inside the bounding box, the result is a small sub-image that contains only one object. Figure 4.2 shows the full image from the video stream (to the left) with a red-colored bounding box containing a vehicle. The right image is the extracted sub-image. The sub-image contains all the pixels that are within the red bounding box shown in the full image. Each of the sub-images are then subjects to image processing and analysis in order to extract bright spot features, which are used for detection and classification of brake lights.

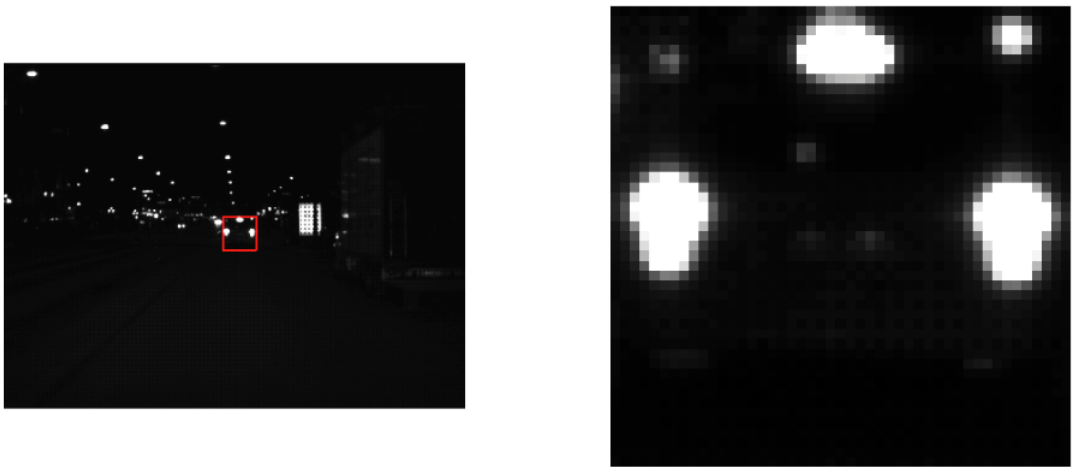

Figure 4.2: Full image (left) and extracted sub-image (right).

4.2 Image processing

The image processing is divided into *Filtering*, and *Thresholding*, presented in the flow chart in Figure 4.3.

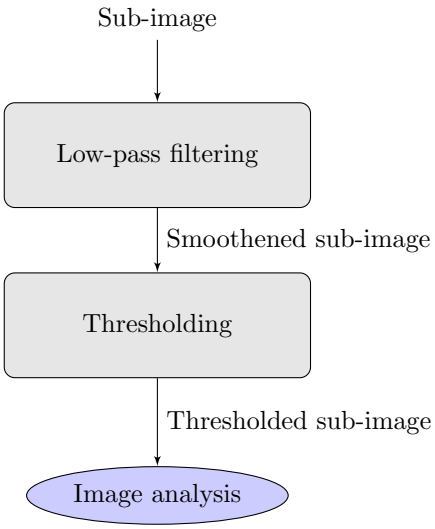

Figure 4.3: Image processing.

4.2.1 Filtering

The image processing to prepare the sub-image for analysis starts with a smoothening in order to remove sharp edges, high frequent noise and smaller light sources, which are possible sources of disturbance in the following image analysis and classification stages. The size of the sub-images depends on the distance to the object, vehicles far away have small bounding boxes while vehicles at close range have larger bounding boxes. Small sub-images can't be processed in the same way as larger images. No filtering is made on small images and the reason for that is that essential information in those images is far more sensitive to low-pass filtering, especially when the rear lights consist of only a few pixels (vehicle at distances over about 70 meters). Low-pass filtering of small images would then, in the worst case, end up with completely removed bright spots and no rear light candidates can be detected. In other word, filtering small images (less than 80x80 pixels) can ruin more than it helps. Larger images (more than 80x80 pixels) are filtered with a Gaussian low-pass filter of size 5x5 and a σ equal to 0.5. The Gaussian low-pass filter is preferred to the average filter, which is rougher in its smoothening [13]. The result of the filtering can be observed in the right image in Figure 4.4.

Figure 4.4: Image low-pass filtering.

4.2.2 Thresholding

Thresholding of the sub-images are used to get rid of bright spots that are not associated with rear lights. Light reflection in the license plate or street lamps with less intense brightness, compared to rear lights, observed next to the vehicle or seen through the windows of the vehicle are two example of bright spots that can be removed or at least reduced in size by thresholding. The rear light analysis showed that even for the short exposure images, the light from the rear lights tend to be saturated, which motivates a high threshold limit of 0.9 (normalized intensity). After the thresholding all pixels with intensity less than 0.9 are set to 0 and all pixels with intensity equal to or greater than 0.9 are set to 1.

The result from the low-pass filtering in the previous step might seem negligible but even a small reduction in intensity or size might due to the high threshold limit lead to either a further size reduction or complete removal of disturbing bright spots. The right image in Figure 4.5 shows the result of the thresholding. One can see all the rear lights (brake lights in this case), a larger light reflection in the bumper and also some smaller bright spots in the rear window, which probably are reflections of street lamps. Comparing the left image in Figure 4.4 to the right image in Figure 4.5, one can see that all the small bright spots not associated with the vehicle's rear lights have been removed or reduced in size. The goal of the image processing is that the rear lights still remain in the image, and hopefully they are easier to distinguish. However, rear lights and other unknown bright spots might merge into a larger semi-true rear light and this needs to be handled in the image analysis part.

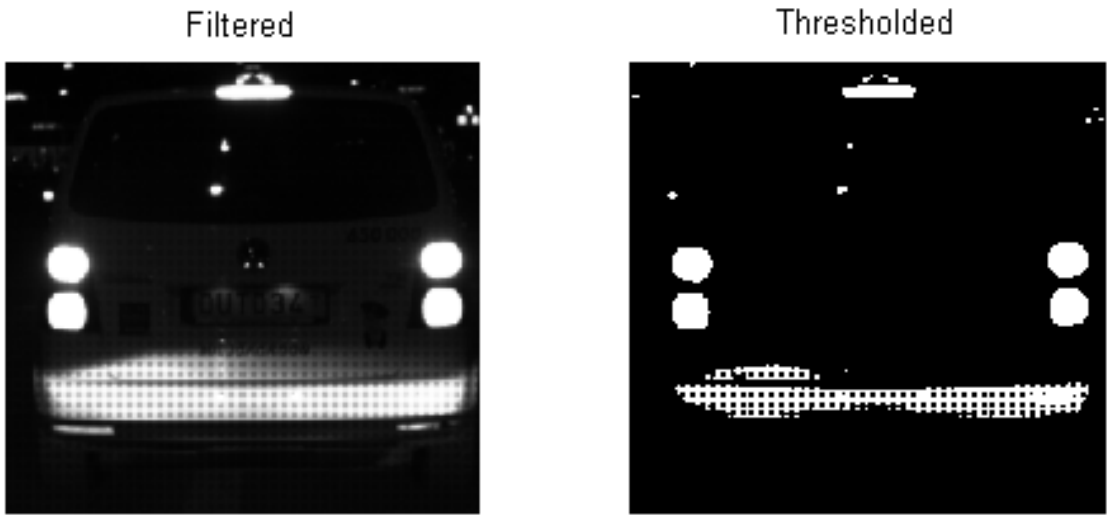

Figure 4.5: Image thresholding.

4.3 Image analysis

The procedure of the image analysis is shown in Figure 4.6. At this stage the image frame is filtered and thresholded and it should contain only relevant bright spots. However, the light conditions in real traffic are varying and light reflections on other vehicles are more intense the closer the distance (the ego-vehicle illuminates close objects more than it illuminates objects further away). The procedure is first to label all the remaining spots, remove undesired spots depending on size and location, the remaining spots are called *candidates* and their features are extracted followed by candidate matching, in which rear-light pairs are found.

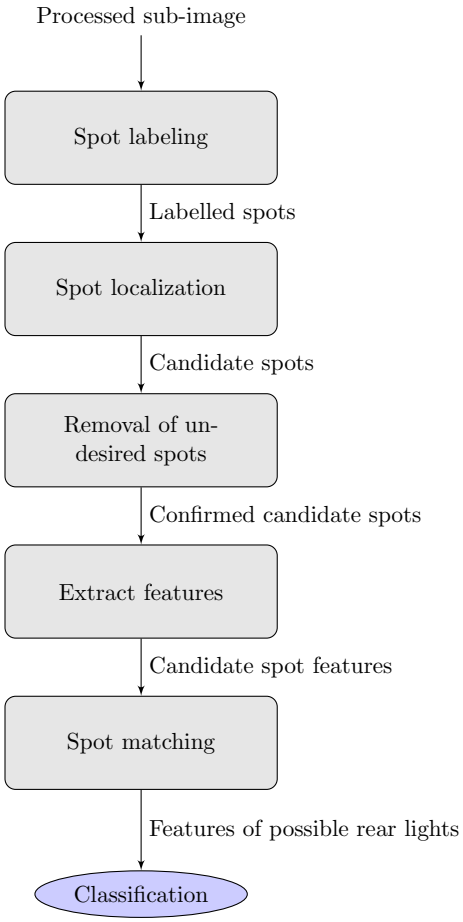

Figure 4.6: Image analysis.

4.3.1 Spot labeling

The first step in this process is to label all the bright spots that are left in the image frame, this is done by finding connected pixels using 8-neighbor connectivity and all connected pixels then form an object, which is assigned a unique number. Each number represents a gray-level intensity, so each bright spot in the image have a unique gray level intensity. The right image in Figure 4.7 below shows the labeled spots represented with different gray-level intensities.

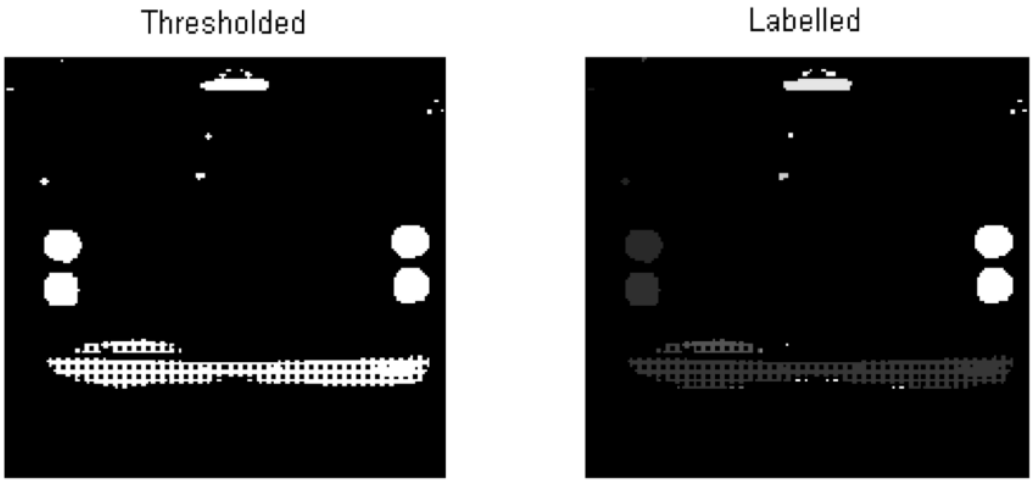

Figure 4.7: Spot labelling.

4.3.2 Spot localization

The first and the third assumption made in the rear light analysis section suggest that rear-lights are positioned one on each side of the rear-end of the vehicle and that the center high mounted stop lamps is centered right between them. All the spots are evaluated based on their x- and y-coordinates in order to sort out the spots that possibly could represent rear-lights. When the localization is completed all remaining spots have been tagged with either "*Left*", "*Right*" or "*Center*". Spots that could not be separated into any of these categories are discarded.

4.3.3 Removal of undesired spots

After the labeling, all pixels that form a spot are assigned a specific value and by computing the sum of all pixels with the same label one can estimate the area of all the spots in the image frame. Bright spots associated with rear lights usually are notably large in size, and constitute at least 0.2% of the total number of pixels in the sub-image (in an 80x80 image, 0.2% corresponds to bright spots of less than 12 pixels). Bright spots smaller than that are treated as noise and can be removed, this is done by setting the value of the pixels belonging to small spots to zero (same as the background). The position of potential rear lights can, according to the assumptions in chapter 3, also be used to remove even large spots located in areas not likely to contain rear lights, a CHMSL can, for instance, not be located below the side rear lights. The images in Figure 4.8 show how small spots and spots not likely to be associated with the vehicle's rear lights have been removed. Only one false or unwanted bright spot (part of the reflection on the rear bumper) is remaining in the image, while the rest of the bright spots can be associated with the vehicles rear lights.

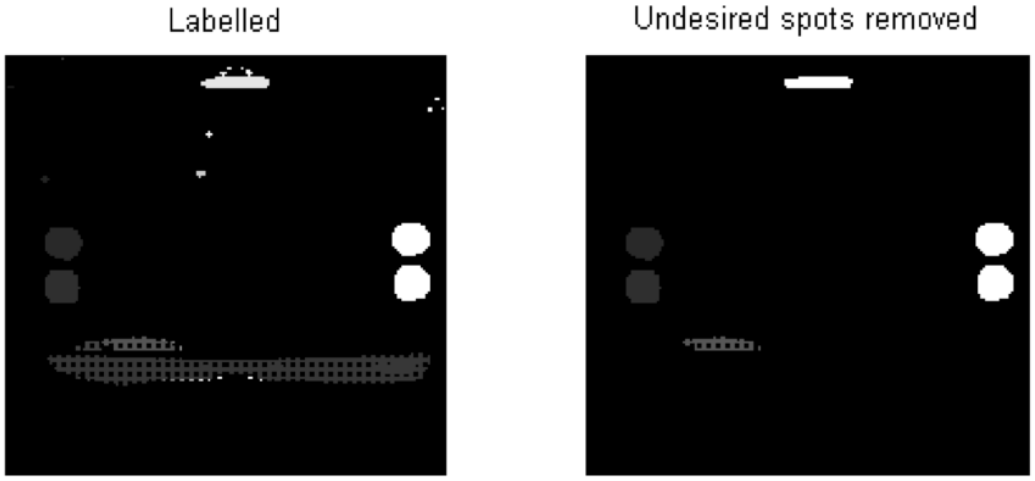

Figure 4.8: Undesired spots removed.

4.3.4 Features

The features of the spots are so called descriptors, i.e. properties used for matching rear lights and further on for classification of rear lights as "*Brake lights*" or "*No brake lights*". The extracted spot features are area (A), intensity ($\bar{I}$) and spot position ($\bar{x}$ and $\bar{y}$).

$$A = N_{spot} \tag{4.1}$$

where N_{spot} in 4.1 denotes the number of pixels in the spot.

$$\bar{x} = \frac{1}{N_{spot}} \sum_{i=1}^{N_{spot}} x_i \tag{4.2}$$

$$\bar{y} = \frac{1}{N_{spot}} \sum_{i=1}^{N_{spot}} y_i \tag{4.3}$$

The average position of the pixels in the spot are estimated in 4.2 and 4.3.

$$\bar{I} = \frac{1}{(x_{max} - x_{min}) * (y_{max} - y_{min})} \sum_{x=x_{min}}^{x_{max}} \sum_{y=y_{min}}^{y_{max}} I(x,y) \tag{4.4}$$

$\bar{I}$ is the average spot intensity, $I(x,y)$ is pixel intensity at coordinates (x,y). The average intensity is computed on a frame around the spot in order to include the spot halo and not only the saturated pixels of the spot. The coordinates of the frame (x,y) are obtained by taking the spot's top (x_{min}), bottom (x_{max}), leftmost (x_{min}) and rightmost (x_{max}) pixel coordinates. Figure 4.9 shows a framed spot with an additional one-pixel wide black boarder, which is not included in the average intensity computation.

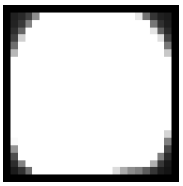

Figure 4.9: An example of a framed spot.

4.3.5 Spot matching

Given the second and the forth assumption about symmetry and visual appearance, one can match candidate spots by comparing their size, average intensity and position. No assumption can be made about the lateral (x-direction) position of the rear-light relative to the bounding box because these boxes might not be centered around the target vehicle, so the rear-light candidates are not matched based on their position in x-direction. Instead, presuming that all vehicles are relatively horizontally aligned one can use the y-position (height) (4.3) of the rear-light candidates when pairing the rear-lights. The intensity (4.4), which is usually saturated for the rear lights, can be used to reject possible side rear light pairs if one of the candidate spots differs in intensity. In the same way candidate spot areas (4.1) can be used in the spot matching, since the assumptions made suggest that rear lights have the same size and intensity. There is a need for lower tolerance levels for the spot matching because, as was mentioned before unknown bright spots can merge with the true rear lights and form a larger contaminated bright spot and there is also a possibility of partial visual obstruction, which might have the opposite effect. The matching criteria are the differences between two candidate spots from left and right side. The thresholds for the matching criteria were estimated by evaluation of a training set of logged video data.

$$\Delta Area < 7.5\%, \quad \Delta\bar{y} < 5\%, \quad \Delta Intensity < 1\%$$

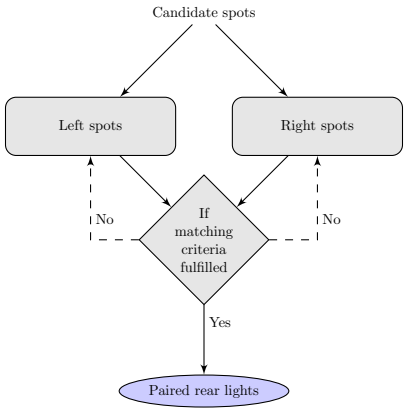

Figure 4.10: Spot matching procedure.

The matching criterias form the basis for the spot matching and the differences in these comparisons must not exceed a certain limit for two spots to match and to form a candidate rear light pair. Center-positioned spots are matched against the right- and left rear lights of the candidate pair. The CHMSL is mounted in the center and as assumption three suggests it is located between the two side rear lights. The CHMSL is matched using the x-position (4.2) of the rear-light pair. According to the fifth assumption in chapter 3, the CHMSL can have different shapes but elongated bright spot are more difficult for external light sources to mimic compared to more circular shaped CHMSLs. This motivates a varying tolerance level for the position offset, and elongated CHMSL are allowed to have up to three times more offset than do the circular ones which are allowed to be positioned with an offset of approximately 12.5% to the center of the rear light pair. A too narrow tolerance level for the CHMSL position obviously causes missed brake light detections while a less narrow tolerance level leads to false brake light detections.
Figure 4.11 shows an example of bad matching rear light candidate pairs, the image to the left illustrates a bright spot reflection on the left side of the bumper (see Figure 4.8) which was not removed in the previous steps. The two images of bright spots in Figure 4.12 on the other hand represents a well-matched rear light candidate pair.

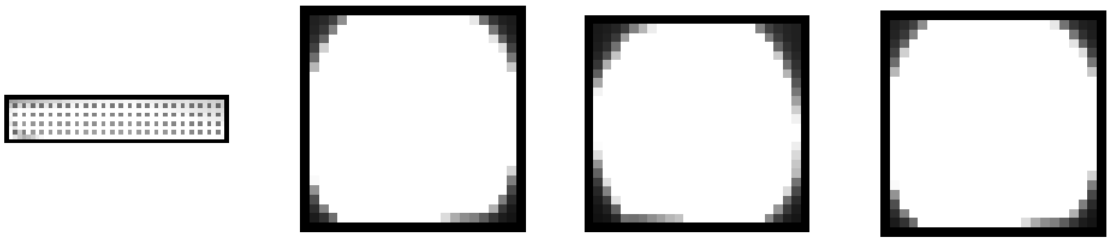

Figure 4.11: Bad match.

Figure 4.12: Good match.

In Figure 4.13 one can see all the steps in the vision algorithm, the top-left image is the original sub-image, top-middle image is the filtered and thresholded sub-image, the top-right image the sub-image with labelled spots (undesired spots are removed), and the bottom images illustrate the side rear lights together with the center high mounted stop lamp (observe that only one of the side rear light pair are presented here).

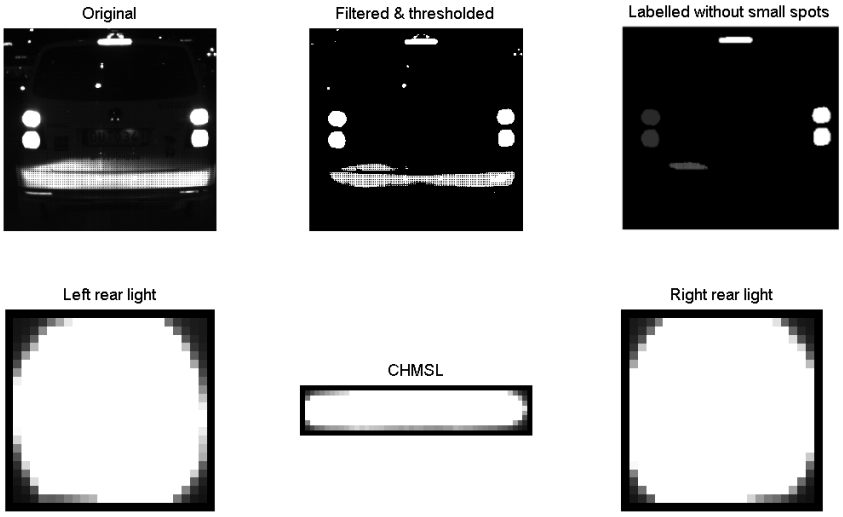

Figure 4.13: Spot matching completed.

4.4 Kalman filter tracking

The bounding boxes that encloses the vehicles of interest in the video frame are not always perfectly centered around their objects, which leads to image analysis issues if one or more rear lights (or brake lights) are partially or completely outside of the bounding box. To solve this issue, Kalman filter tracking of the rear lights is used to update the coordinates of the bounding box to better fit its object. The Kalman states being tracked are the leftmost- and rightmost coordinates of the side rear-lights. The model of the position estimation of the rear lights is based on a constant acceleration model, which are more accurate than the simpler constant speed model if Kalman parameters are properly set [14]. The model is described with a difference equation of first order (here index k represents the video frame index) [15]:

$$\boldsymbol{x}(k+1) = \boldsymbol{A}\boldsymbol{x}(k) + \boldsymbol{w}(k) \tag{4.5}$$

$$\boldsymbol{y}(k) = \boldsymbol{C}\boldsymbol{x}(k) + \boldsymbol{v}(k) \tag{4.6}$$

The state- and measurement noise ($\boldsymbol{w}$ and $\boldsymbol{v}$) are assumed to be normally distributed zero mean random variables independent of $\boldsymbol{x}$ [15].
The equations of motion used in the model of the rear light movement is presented here below. Equation 4.7 describes the position of a moving object with a constant linear acceleration and equation 4.8 describes the velocity affected by the same acceleration.

$$x = x_0 + \dot{x}t + \frac{\ddot{x}t^2}{2} \tag{4.7}$$

$$\dot{x} = \dot{x}_0 + \ddot{x}t \tag{4.8}$$

The state vector $\boldsymbol{x}$ (4.9) contains all the states in the Kalman filter, one such vector for each of the side rear light.

$$\boldsymbol{x}(k) = \begin{bmatrix} x(k) \\ \dot{x}(k) \\ \ddot{x}(k) \\ y(k) \\ \dot{y}(k) \\ \ddot{y}(k) \end{bmatrix} \tag{4.9}$$

The state transition matrix $\boldsymbol{A}$ (4.10) is the model used for prediction of the states.

$$\boldsymbol{A} = \begin{bmatrix} 1 & dt & \frac{dt^2}{2} & 0 & 0 & 0 \\ 0 & 1 & dt & 0 & 0 & 0 \\ 0 & 0 & 1 & 0 & 0 & 0 \\ 0 & 0 & 0 & 1 & dt & \frac{dt^2}{2} \\ 0 & 0 & 0 & 0 & 1 & dt \\ 0 & 0 & 0 & 0 & 0 & 1 \end{bmatrix} \tag{4.10}$$

The measurement matrix $\boldsymbol{C}$ (4.11) is presented here below and it represents the states that are being measured (the x and y coordinates of the rear lights).

$$\boldsymbol{C} = \begin{bmatrix} 1 & 0 & 0 & 0 & 0 & 0 \\ 0 & 0 & 0 & 1 & 0 & 0 \end{bmatrix} \tag{4.11}$$

The process noise is assumed to be almost zero (but not zero to avoid matrix inverting issues) and the ratio between covariance matrices of the measurement noise (R) and the process noise (Q) is large, which means that the Kalman filter becomes more smooth than responsive. For the y-positions of the rear lights the R/Q-ratio is even larger to make it more smooth and less responsive compared to the tracking of the lateral position of the rear lights. The reason for having a more responsive tracking of the lateral position of the side rear lights is that vehicles tend to travel more laterally than horizontally.
The Kalman filtered positions of the rear lights are then used to adjust the succeeding bounding boxes so that they enclose the subject vehicle in a more optimized way. Each bounding box update is using the old bounding box coordinates (bb) as reference. The height of the bounding box ($\Delta Y = bb_{bot} - bb_{top}$) remains unchanged but the box is centered around the side rear lights. The coordinate of the top position of the bounding box is updated by adding the y-position of the side rear lights' top pixel position to the

old bounding box top coordinate and then subtract half the bounding box height (see expression 4.12).

$$bb^*_{top} = bb_{top} + y - \frac{\Delta Y}{2} \tag{4.12}$$

After the top coordinate of the bounding box is updated according to expression 4.12, the bottom coordinate of the bounding box can be updated using the new top coordinate and add the height of the original bounding box (see expression 4.13).

$$bb^*_{bot} = bb^*_{top} + \Delta Y \tag{4.13}$$

In this way the height of the original bounding box is preserved and the bounding box is vertically centered around the subject vehicle in the sub-image.
The lateral position of the bounding box is adjusted in a similar way, although the width is not kept the same but it is slightly increased to ensure that no side rear lights ends up outside the bounding box even after the first horizontal adjustment of the Kalman filtered positions, which could be the problem if the original bounding box is too narrow from the beginning. Once again the old bounding box coordinates are being used as a starting point, where the old leftmost bounding box coordinate (bb_{left}) together with the coordinate of the leftmost pixel position of the left side rear light (x_{left}) forms the new leftmost coordinate of the adjusted bounding box (bb^*_{left}), (see expression 4.14).

$$bb^*_{left} = bb_{left} + x_{left} \tag{4.14}$$

The rightmost coordinate of the bounding box is then updated by adding the rightmost pixel position of the right side rear light, x_{right} to bb^*_{left} (see expression 4.15).

$$bb^*_{right} = bb^*_{left} + x_{right} \tag{4.15}$$

Now the horizontal position of the bounding box is suppose to be centered around the vehicle in the sub-image but a margin (2.5% of the width) is added on each side to ensure complete coverage of the side rear lights.
The occurrence of critically misaligned bounding boxes is low (a rough estimation would be less than 5% of all events), however in such a case it is most likely for the algorithm to fail to detect brake lights or it might even report false brake light detections if other unknown light sources, that appear in the sub-image look like brake lights. Figure 4.14 here below shows a good example in which the Kalman filtering manage to adjust the bounding box so that all rear lights including the center high mounted stop lamp are visible. The result is a successful brake light detection, which was not the case when using the original bounding box. The red markers in the right image show the Kalman tracking of the side rear lights.

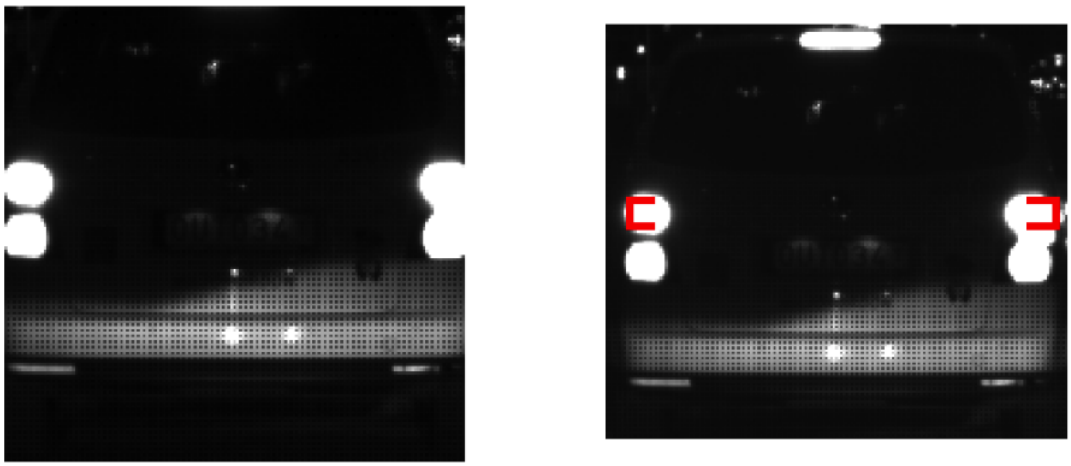

Figure 4.14: Misaligned bounding box (left) and adjusted bounding box (right).

4.5 Decision-making procedure

The decision-making procedure is divided into two steps. First the candidate rear lights are classified as *brake lights* or *no brake lights* by pattern recognition and secondly an additional method for brake light confirmation is used to make the decision-making more robust and less sensitive to disturbances.

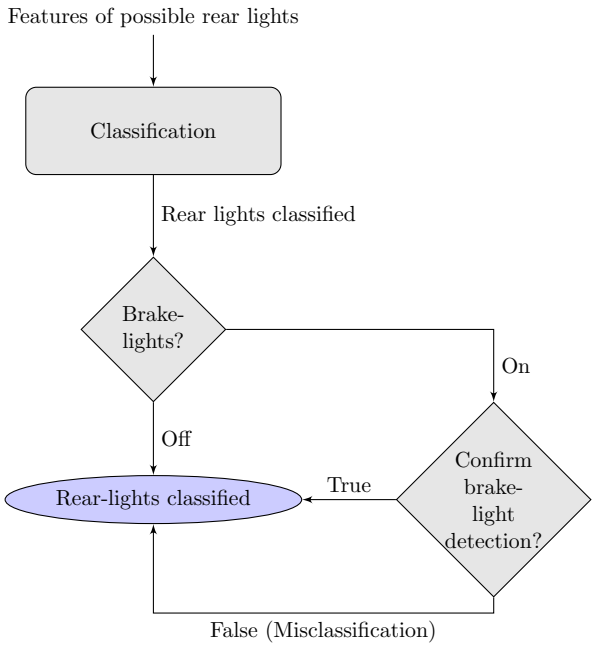

Figure 4.15: Decision-making procedure.

4.5.1 Pattern recognition

The classification is the process in which an object with certain features $\boldsymbol{X}$ is predicted to belong to a specific class. Before going more into the concept of pattern recognition and classification it is necessary to study the features of the rear lights extracted in the vision algorithm that are to be recognized and which the classification will be based upon.

Rear light features

In this section three plots of the rear lights features are presented. The features are extracted from samples in a training set of single images of rear lights.
As was already noticed and mentioned in the rear light analysis in chapter 3, the difference in brightness intensity between brake lights and normal rear lights is quite small and the problem here is the intensity saturation. This is shown in Figure 4.16, which is a scatter plot of all features of all candidate rear lights in the training set. The average intensity of all matched rear light spots is plotted against the total area of all the matched rear light spots for each of the samples. One can see that all samples, with or without brake lights seem to have similar intensity while the size of the lights is larger for the samples of braking vehicles.

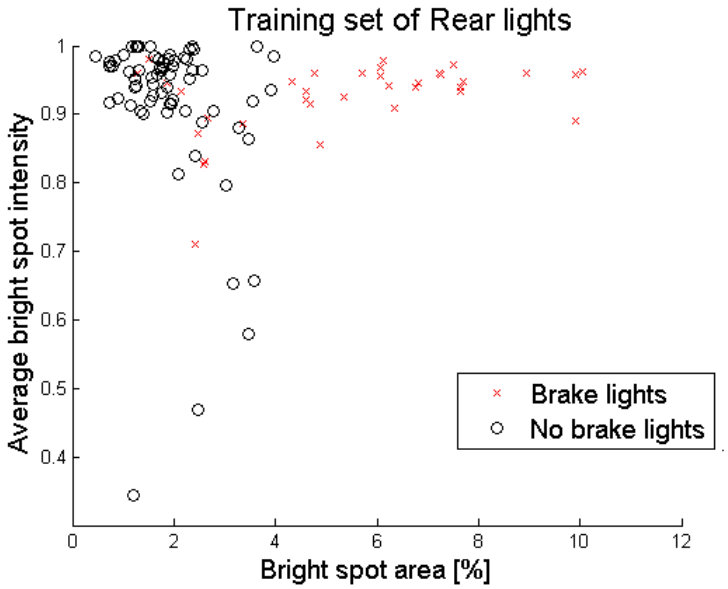

Figure 4.16: Scatter plot of rear light features.

Another approach was to use the accumulated intensity, i.e. the sum of the intensity for all matched candidate rear light spots, the result is presented in Figure 4.17. and as one can see the there is a more clear distinction between brake lights and no brake lights.

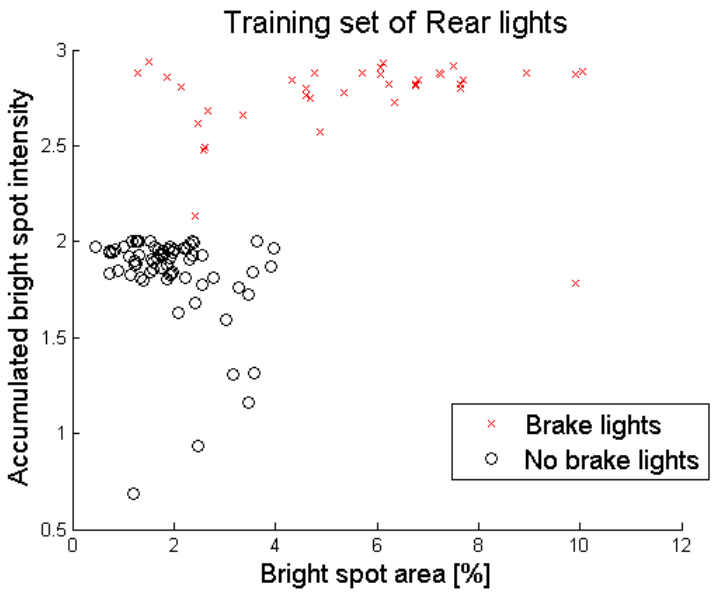

Figure 4.17: Scatter plot of rear light features (accumulated intensity).

According to the third assumption in chapter 3, all cars are assumed to have a center high mounted stop light, which is lit during braking. By using the accumulated intensity of the rear lights and adding a weighting factor of 2 to the features of the CHMSL (enhancing its features) will lead to an increased margin between the brake lights and normal rear lights, which can be seen in Figure 4.18.

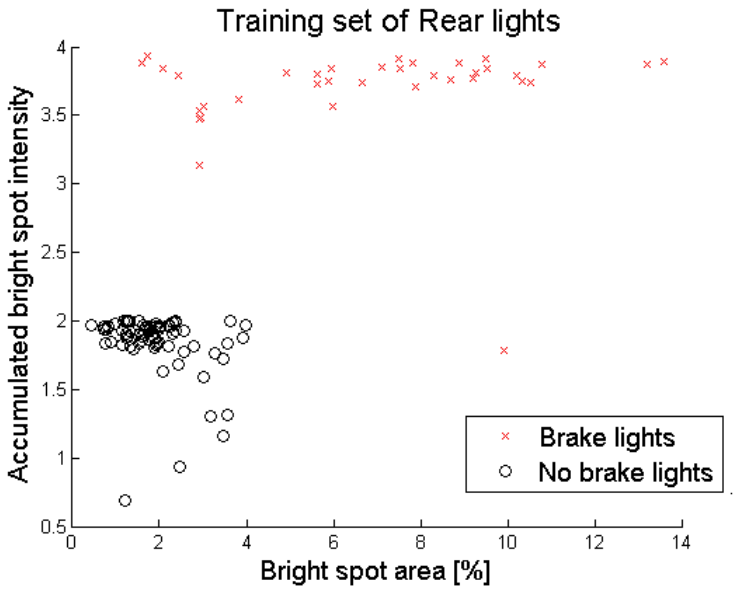

Figure 4.18: Scatter plot of rear light features (weighted CHMSL features)

The features that the object recognition will be based on are the total accumulated intensity (i.e. the total illumination of the rear lights, which is dependent on the number of matched bright spots) and the total area of the rear lights.

Discriminant analysis

Linear Discriminant Analysis (LDA) and *Quadratic Discriminant Analysis* (QDA) are methods to identify linear and non-linear combinations of features that separates objects of different classes, like for instance weed seeds [10]. One assumes a given number of classes and the objective is to assign an unclassified object to one of the classes. LDA and QDA are supervised pattern recognition methods, in that sense a training set of objects with certain features belonging to a known class is used to train the classifier (also called *supervised learning*).
$\boldsymbol{X} \sim \mathcal{N}(\boldsymbol{\mu}_i,\boldsymbol{C}_i)$ is a multivariate normally distributed d-dimensional column vector with density function 4.16. The dimension d depends on the number of features used in the classification, in this case two features are used thus a two-dimensional density function [10, 16].

$$f_{\boldsymbol{X}}(\boldsymbol{x}) = \frac{1}{2\pi\sqrt{det\boldsymbol{C}}} e^{-\frac{1}{2}(\boldsymbol{x}-\boldsymbol{\mu})^T \boldsymbol{C}^{-1}(\boldsymbol{x}-\boldsymbol{\mu})} \tag{4.16}$$

The symbol $\boldsymbol{x}$ represents features of an unclassified object. $\boldsymbol{\mu}_i$ are expectation vectors and $\boldsymbol{C}_i$ are covariance matrices of the features in class i. Class 1 is "*Brake lights*" and class 2 represents "*No brake lights*". π_i is a priori probability for an object to belong to class i.

The probability of misclassification is minimized by preferring class 1 to class 2 when [10, 16]:

$$\pi_1 f_1(x) > \pi_2 f_2(x) \tag{4.17}$$

The main difference between LDA and QDA is that in LDA one assumes the covariance matrices $\boldsymbol{C}_i$ to be of the same structure by pooling them together (4.18).

$$\boldsymbol{C} = \frac{1}{(n_1 + n_2 - 1)} \sum_{i=1}^{2} (n_i - 1)\boldsymbol{C}_i, \tag{4.18}$$

n_1 and n_2 are the number of "*Brake lights*" and "*No brake lights*" samples used in the classifier training. The result is a linearization of 4.17 i.e. the terms to the left of the exponential term in 4.16 are cancelled out, which leads to a linear classification expression (4.19):

$$\pi_1 e^{-\frac{1}{2}(\boldsymbol{x}-\boldsymbol{\mu}_1)^T \boldsymbol{C}^{-1}(\boldsymbol{x}-\boldsymbol{\mu}_1)} > \pi_2 e^{-\frac{1}{2}(\boldsymbol{x}-\boldsymbol{\mu}_2)^T \boldsymbol{C}^{-1}(\boldsymbol{x}-\boldsymbol{\mu}_2)} \tag{4.19}$$

The expression is simplified by taking the natural logarithm of both sides and rearranging the equation:

$$-\frac{1}{2}(\boldsymbol{x}-\boldsymbol{\mu}_1)^T\boldsymbol{C}^{-1}(\boldsymbol{x}-\boldsymbol{\mu}_1)+\frac{1}{2}(\boldsymbol{x}-\boldsymbol{\mu}_2)^T\boldsymbol{C}^{-1}(\boldsymbol{x}-\boldsymbol{\mu}_2)>\ln\frac{\pi_2}{\pi_1} \tag{4.20}$$

If we assume the probability of both classes to be equal the final expression then is to prefer class 1 to class 2 when:

$$(\boldsymbol{\mu}_1-\boldsymbol{\mu}_2)^T\boldsymbol{C}^{-1}(\boldsymbol{x}-\frac{1}{2}(\boldsymbol{\mu}_1+\boldsymbol{\mu}_2))>0 \tag{4.21}$$

In the case of LDA, the decision-boundary is a straight line (equation A.2) in the x and y-plane, where x and y represents the feature vector $\boldsymbol{x}$, thus area and intensity, respectively. The derivation of the decision-boundary can be found in Appendix A.

In the non-linear case (QDA), the covariance matrices are not pooled, which gives the following expression for classification and class 1 is preferred to class 2 when:

$$(\boldsymbol{x}-\boldsymbol{\mu}_2)^T\boldsymbol{C}_2^{-1}(\boldsymbol{x}-\boldsymbol{\mu}_2)-(\boldsymbol{x}-\boldsymbol{\mu}_1)^T\boldsymbol{C}_1^{-1}(\boldsymbol{x}-\boldsymbol{\mu}_1)-\ln\frac{det(\boldsymbol{C}_1)}{det(\boldsymbol{C}_2)}>0 \tag{4.22}$$

Just like for the LDA, a decision-boundary for the QDA can be derived. This time the decision-boundary is a quadratic function (equation A.6) derived from equation 4.22, see Appendix A for further information.

Confidence level

Several consecutive video frames containing a vehicle with classified brake lights are more likely to be represent a true brake light detection compared short brake light events that are no longer than a couple of frames. Such short events are more likely to be false brake light detection, caused by interfering external light sources that by mistake were matched as a CHMSL. The number of consecutive frames with classified brake lights is used as a simplified kind of confidence level of the classification. This means that short false brake light detections will have a low confidence level while longer events of brake light detection have a high confidence level. High confidence is obtained after 5 consecutive brake light classifications and an interruption, i.e. rear lights not classified as brake lights will directly lead to low confidence.

4.5.2 Brake light confirmation

The classification based on the pattern recognition described in the previous section is carried out on every bounding box sub-image. It is the first step in the brake light detection. There is a large variance in mounting position, size and shape for rear lights (and especially the CHMSL) depending the car model. In order to detect brake lights on any kind of vehicle (with a CHMSL) in the field of view the tolerance levels need to be low. In addition to that, the perspective are also skewed for brake lights on vehicles in adjacent lanes which also motives low tolerance levels. Low tolerance levels lead to increased number of misclassifications because external light sources similar to

rear lights in size, shape and position become more difficult for the vision algorithm to reject. If one of these external light sources can be mistaken for a CHSML the result will be a false brake light detection. One can distinguish two types of false detections, namely long and short false detections. Short false detections are caused by temporary interference of external light sources, such as street lamps (stationary light sources). If the vehicle moves, then the relative motion between the stationary external light and the rear lights lead to only a short false brake light detection. Long false detections are caused by interfering light sources similar to a CHMSL observed over a longer period of time. Examples of this can be rear lights of other vehicles ahead, seen through the windows of the subject vehicle. Another example is when multiple light sources merge and form a more or less constant light inside the bounding box (head lights of oncoming vehicles on the motorway, see Figure 6.5).
One way of tackling the problem with short false detections is to observe the area and intensity of the possible rear lights and search for relatively large changes yet avoiding the influence of temporary disturbing lights that cause false detections. We define two features, μ_{short} - short average, and μ_{long} - long average, along with their difference $\Delta\mu$ (4.23, 4.24, and 4.25).

$$\mu_{short}(k) = \frac{1}{5} \sum_{i=k-4}^{k} I(i) \cdot A(i) \tag{4.23}$$

$$\mu_{long}(k) = \frac{1}{10} \sum_{i=k-9}^{k} I(i) \cdot A(i) \tag{4.24}$$

$$\Delta\mu(k) = \mu_{long}(k) - \mu_{short}(k) \tag{4.25}$$

where I and A are the features described in the beginning of section 4.5.1, i.e. the intensity and the area for all matched spots in the bounding box (the sub-image). The index k represents the frame number. The short average (μ_{short}) will react more rapidly to a change in A or I, compared to its longer counterpart (μ_{long}). By observing $\Delta\mu$ one can notice a relatively large peak when the brake lights have been lit while for temporary disturbing lights that cause false detections will result in only a smaller peak, as can be seen in the middle plot in Figure 4.19. In this way one can look for such a large peak when brake lights have been classified by the classifier, i.e. after brake lights have been detected a large peak in $\Delta\mu$ will follow in case of a true brake light detection, otherwise one assumes the classifier to be wrong and the misclassification is ignored and no brake lights are reported.

This makes the brake light confirmation insensitive to short disturbances, since the average values of the signal will not be able to ”build up” their average values as much as for a true status change, when the value of the signal is either constantly high or constantly low. There is however a backside to this method. The peak value that $\Delta\mu$ needs to exceed varies depending mainly on the width of the bounding box, which in turn is range (to the object) dependent. The size of rear lights of a vehicle does not

change at the same rate as the size of the bounding box when the object gets closer to the ego-vehicle. The peak threshold $T_{\Delta\mu}$ have been estimated by interpolation of peak values from different vehicles and bounding box widths found in the training sample (further information can be found in Appendix A):

$$T_{\Delta\mu} = 9.8 - 0.019 \cdot (bb_{right} - bb_{left}) \tag{4.26}$$

To ensure $T_{\Delta\mu}$ to be exceeded it is decreased to 75% of its original value. However, if the confidence level of the brake light detection is high (many consecutive brake light classifications), the peak value of $\Delta\mu$ does not have to exceed any limit for the brake light to be confirmed as true brake lights. This is to ensure that even brake lights of vehicles with relatively small brake lights will be detected and not ignored because of the lower value of $\Delta\mu$.
The issue concerning disturbing light sources that are observed and classified as brake lights for a longer period of time (longer than four image frames) still remains and it will cause false detections. One way of dealing with this problem is to look for an increased size of the side rear lights, which would correspond to lit brake lights. ΔA_{side} will represent the size difference of the side rear lights between every frame. As was mentioned in the end of chapter 3, if there are additional side brake lights (only lit during braking) then the total size of the side brake lights could be twice the size of the rear lights while in the worst case ΔA_{side} might not be greater than 12.5%. This means that the risk for noise to influence and cause a false triggering of the ΔA_{side} is larger for vehicles with small rear lights with no additional side brake lights. The triggering limit for ΔA_{side} to approve a brake light classification is:

$$T_{\Delta A_{side}} = 0.125 \tag{4.27}$$

The plots in Figure 4.19 show the brake light detection and the two confirmation methods. The top plot is the brake light detection based on the classifier. The middle plot illustrates $\Delta\mu$ (blue line) and $T_{\Delta\mu}$ (black, dashed line). The bottom plot shows the ΔA_{side} (blue line) with its corresponding threshold limit, $T_{\Delta A_{side}}$ (black, dashed line).

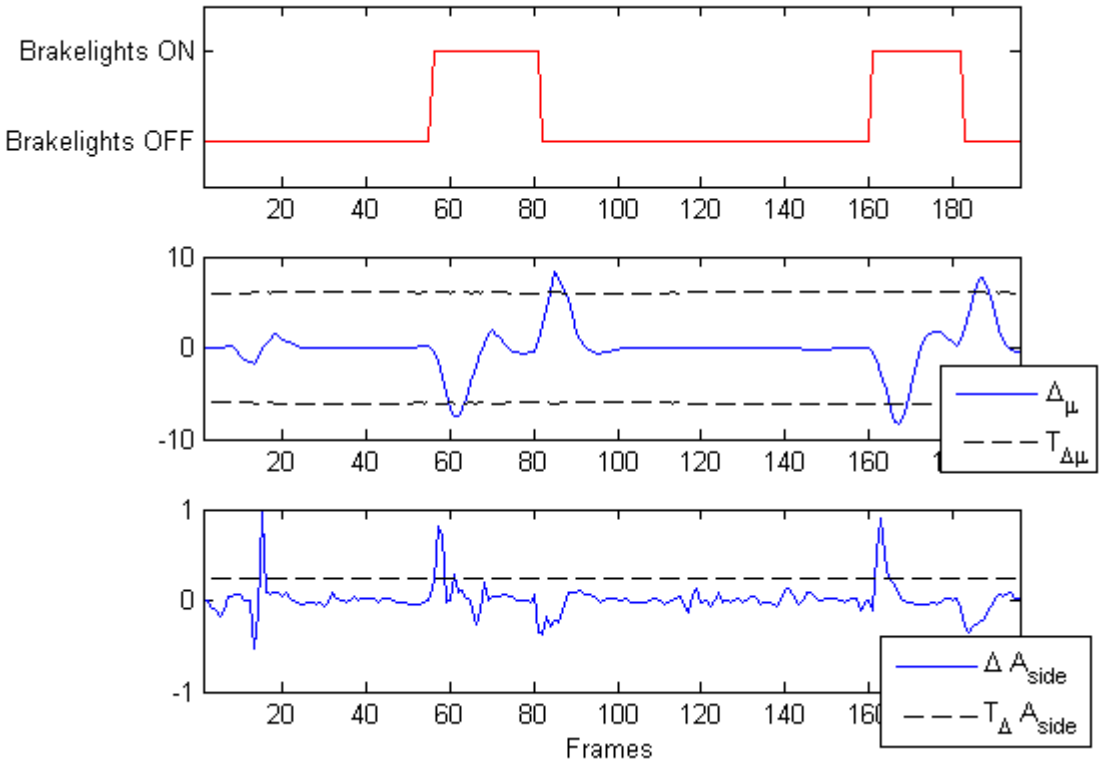

Figure 4.19: Brake light detection and confirmation.

The upper plot shows the output from the classifier (QDA) and two brake lights events can be seen between frames 57-80 and 160-180. A true brake light detection would generate a large peak of $\Delta\mu$, and as the plot in the middle shows, two clear peaks that exceed $T_{\Delta\mu}$ can be seen about three frames after the first frame of the two classified brake light events in the upper plot. One can also see two peaks for when the brake lights release, i.e. the end of the braking event. The plot in the bottom of Figure 4.19 shows ΔA_{side} and there are three distinctive peaks exceeding the threshold level. Two of the peaks are when the brake lights were lit, and those peaks almost reaches 1.0 which means that the side brake lights are almost twice as large as the rear lights. The first peak, at frame 15, is because the ego vehicle went over a speed bump which lead to a quick pitching motion that caused the vehicle ahead (and its rear lights) to almost completely disappear out of field of view. In summary, the video sequence described in Figure 4.19 is an example of the decision-making procedure where two brake light events were found and confirmed true.
The final part of the brake light detection algorithm, with a more extensive description of the brake light confirmation method (the two rightmost decision blocks) is presented in Figure 4.20. The brake light detection algorithm has a hierarchic classification approach

and each block in Figure 4.20 represents a classification method that uses the extracted features in different ways in order to detect, classify and confirm true brake light events.

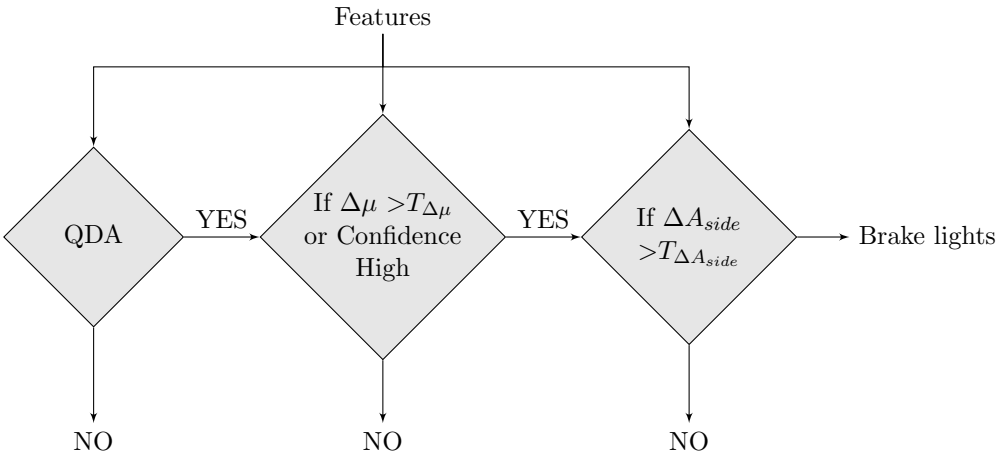

Figure 4.20: Brake light detection algorithm

5

Results

This chapter contains the results or the performance of the main parts presented in the methodology chapter. First to be presented is the reliability of the vision algorithm, i.e. how often the image analysis algorithm finds and differentiates all rear lights of a vehicle, and then the error rate of the classification methods is evaluated followed by an evaluation of the complete brake light detection algorithm. The so called *hold out* method was used to divide a data set of random single image frames of vehicles with and without lit brake lights into a training set and a validation set. The training set was used to estimate threshold values for spot matching and the extracted features were used in the training of the classifier. The vision algorithm and the classifier were then tested on the validation set. The samples in the two data sets don't contain disturbing light sources that easily could be mistaken for a vehicle's brake light. The final evaluation of the complete brake light detection algorithm is made on a large set of video data. The last section in this chapter is a presentation of the support tool developed to make the sensor system output evaluation less time consuming and more efficient.

5.1 Vision algorithm reliability test

The vision algorithm is the image processing and image analysis combined and in this section the performance of vision algorithm of the system is evaluated. A reliability test is performed on a training- and a validation set containing images of vehicles to show how well the algorithm manage to differentiate bright spots associated with rear lights. The success rate of the vision algorithm is a measure of how reliable the algorithm is on detecting the correct spots associated with rear lights. The *Exact* method also called the *Clopper-Pearson interval*, which is a one-sided binomial confidence interval was used to calculate the reliability of the vision algorithm. In Table 5.1 the performance or the reliability of the vision algorithm is presented for the training- and the validation set.

Further information about the reliability computation can be found in Appendix A. The vision algorithm was not able to analyze one of the samples in the training set correctly while 100% of the samples in the validation set was successfully analyzed and all rear lights were found. The failed sample from the training set is shown in Figure 5.1. The reason to the failure is that the vehicle in the sample image is observed from a long distance, which means a small bounding box and the rear lights of the vehicle are more all less completely merged and the vision algorithm succeeds only in distinguishing two of the three lights. In Figure 5.2 a successfully analyzed training sample is shown, here the vision algorithm manage to find all three lights associated with the vehicle's rear lights.

Table 5.1: Reliability test results

Set	Number of trails (N)	Number of successes	Reliability (CL 95%)
Training	105	104	95.6%
Validation	66	66	95.3%

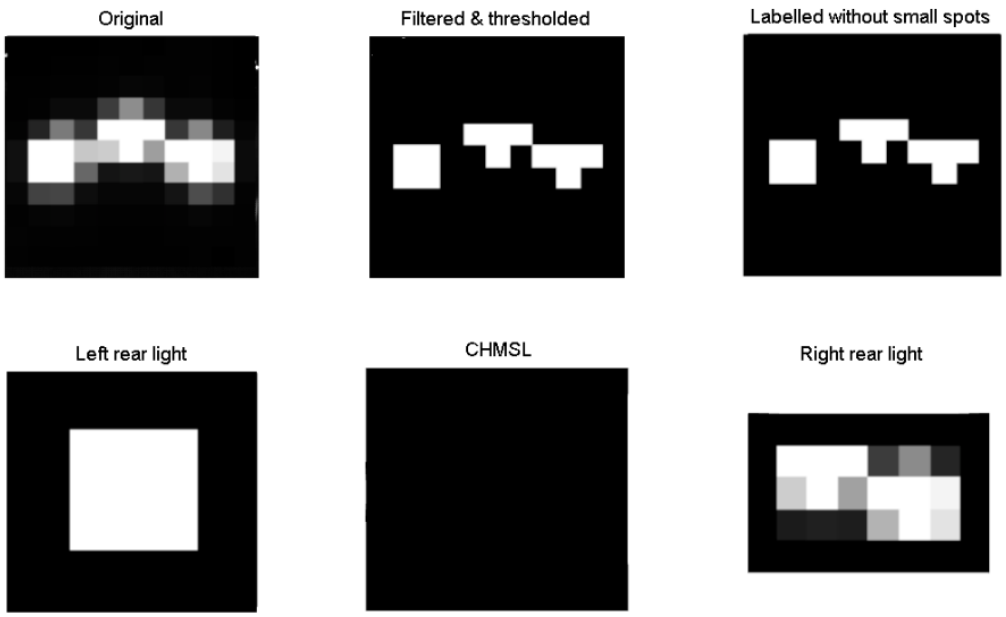

Figure 5.1: Failed training sample.

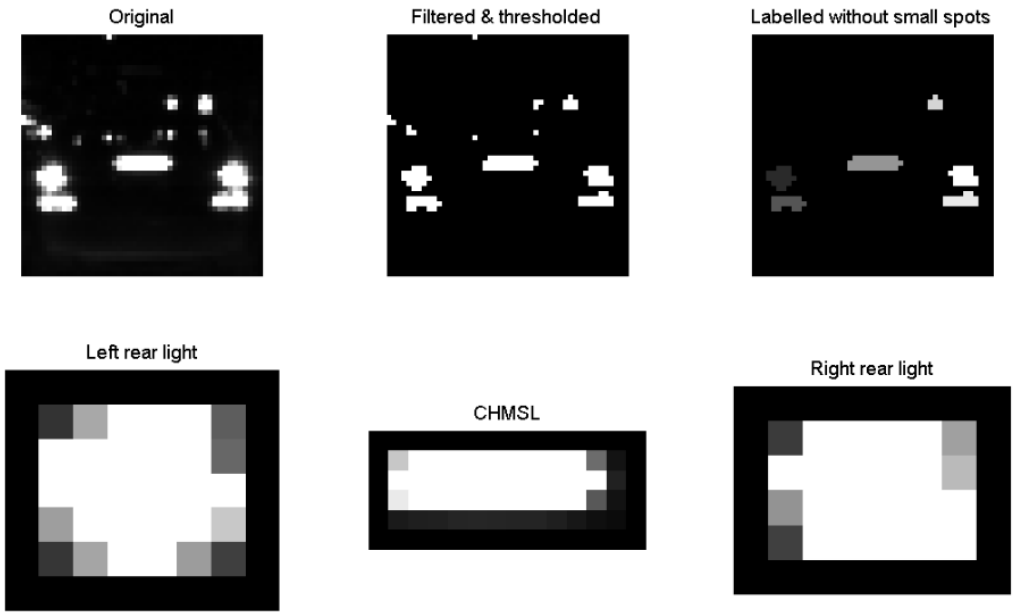

Figure 5.2: Successful training sample.

5.2 Classification error rate

In this section the performance of the classification is evaluated in terms of number of errors, i.e. misclassifications. The two sample sets (training and validation) are being subjects for the brake light classification. Table 5.2 shows the number of misclassifications and the error rate for the two methods (LDA and QDA), and for the two sample sets. In the last four rows in Table 5.2 the vision algorithm weighting the different rear lights, meaning that a CHMSL, which is associated with braking is valued higher than the other two (side) brake lights. So by weighting the features of the CHMSL (increasing the intensity and the area of these spots) one increases the margin between ordinary rear lights and brake lights as can be seen in Figures 5.4 and 5.6. This leads to a more distinctive differentiation between the two classes and the number of misclassifications is reduced, which Table 5.2 shows. Samples found below the decision-boundaries are classified as ”Rear lights” while samples above the decision-boundaries are classified as ”Brake lights”.

Table 5.2: Classification error rate

Method	Set	Number of trails (N)	Misclassifications	Error rate
LDA	Training	105	1	0.95%
LDA	Validation	66	0	0.00%
QDA	Training	105	1	0.95%
QDA	Validation	66	0	0.00%
LDA	Training (weighted)	105	1	0.95%
LDA	Validation (weighted)	66	0	0.00%
QDA	Training (weighted)	105	0	0.00%
QDA	Validation (weighted)	66	0	0.00%

In this case both LDA and QDA perform well and they fail on classifying the same sample as Figure 5.3 shows. When weighting the features (i.e. enhanced features) of the CHMSL spots, hence increasing the margin between the two classes, only the sample that failed in the vision part (Figure 5.1) becomes separated from the other two, more distinct groups yet the QDA manages to correctly classify it, which can be observed in Figure 5.4.

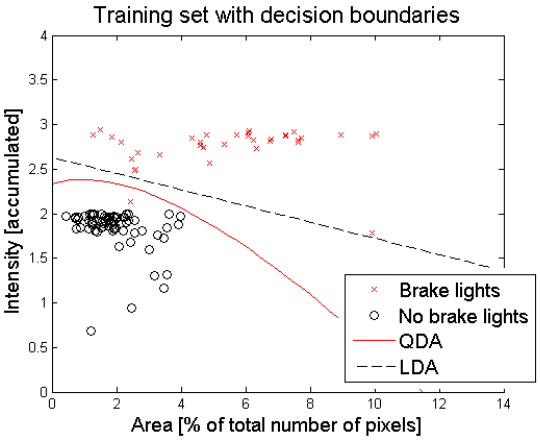

Figure 5.3: Training set

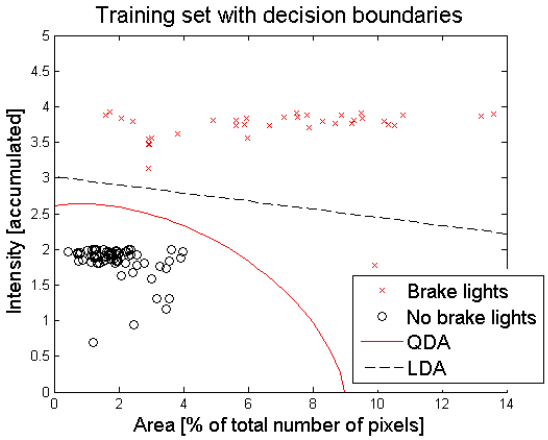

Figure 5.4: Training set (weighted CHMSL features)

In Figures 5.5 and 5.6 the decision-boundaries of the LDA and the QDA are plotted together with the rear light samples in the validation set.

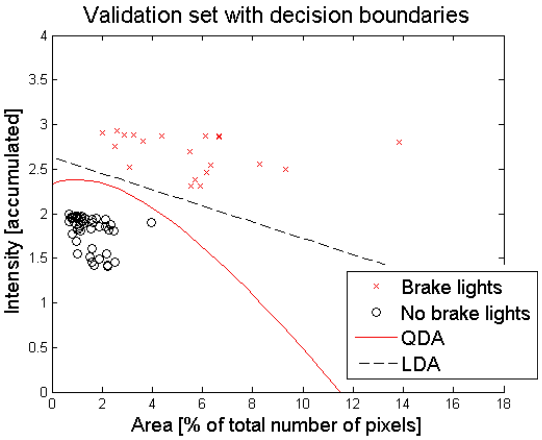

Figure 5.5: Validation set

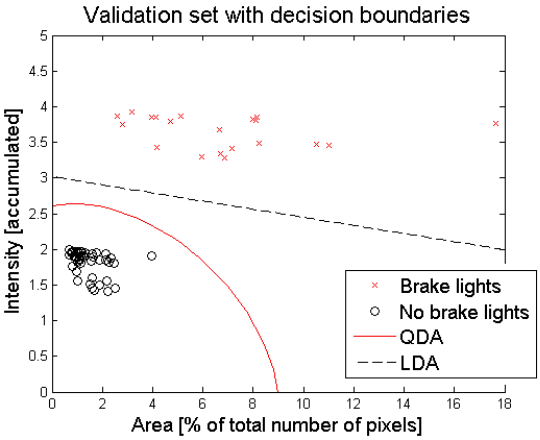

Figure 5.6: Validation set (weighted CHMSL features)

5.3 Brake light detection evaluation

The results presented in this section **do not** describe the performance of the actual sensor system. It is an evaluation of the proposed brake light detection algorithm developed in this thesis project.
The brake light detection algorithm has been tested and evaluated on a large data set. Over 900 minutes of video data have been assessed and over 140.000 sub-images were processed in about 190 minutes. 432 braking events were detected. 65 out of these 432 events were false positives, which corresponds to a false detection rate of about 15%. According to manual ground truthing about 15 events were only partly detected by the brake light detection algorithm (due to temporary visual obstruction) and four events were completely missed. The missed detection rate is only about 1%.

Table 5.3: Brake light detection

	Event	No Event
Output	367	65
No Output	4	927

The sensitivity of the brake light detection algorithm is its ability to correctly detect brake lights:

$$Sensitivity = \frac{TruePositives}{TruePositives + FalseNegatives} \tag{5.1}$$

The sensitivity is 98.9%.
The specificity of the brake light detection algorithm is its ability to correctly not detect

brake lights:

$$Specificity = \frac{TrueNegatives}{TrueNegatives + FalsePositives} \tag{5.2}$$

The specificity is 93.4%.

5.4 The support tool

The support tool is a graphical user interface (GUI) to make it easier to evaluate the sensor output according to the requirements. The events found by the brake lights detection algorithm will be used to evaluate missed events by the sensor system and the events found by the sensor system will be evaluated as true or false events. Figure 5.7 shows the GUI and as one can see it is possible to browse between events, watch the entire event or just step through it frame by frame and also evaluate frames before and after the actual events. Once the evaluation is done, the user annotates the event by clicking on either ”Brake lights ON” or ”Brake lights OFF” followed by either ”PASS”, ”FALSE” or ”MISSED” depending on the output of the sensor system shown in the plot in the upper-right corner.

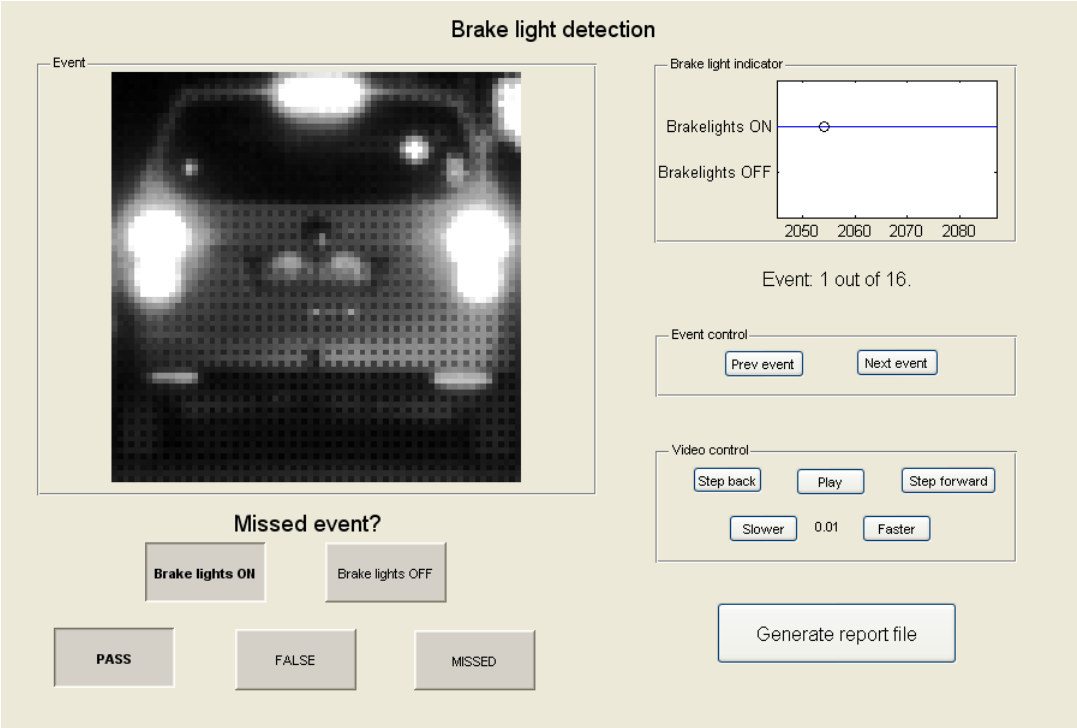

Figure 5.7: The support tool (GUI).

When all events have been annotated the user can click on the ”Generate report”-button to generate an excel sheet containing information about the events and also

statistics of the performance of the output (see Figures 5.8 and 5.9). Figure 5.8 shows an example of how the events evaluated with the support tool are presented in an excel sheet.

	A	B	C	D	E	F
1	DVL File Name	Vision Track id	Vision start index	Vision end index	Range	Annotatio
2	1	2	2045	2087	21.8	OK
4	2	9	2339	2366	40	OK
6	3	10	1873	1881	30.2	FALSE
8	4	9	1	29	34.6	OK
9	5	9	94	309	15.7	MISSED
10	6	9	360	397	6.7	MISSED
13						
14						
15						

Figure 5.8: Excel report example 1 - Events.

In Figure 5.9 you can find the statistics based on the events in the previous figure.

	A	B	C	D
1				
2	**Description**	**Events**	**%**	
3	Total	6	100.00	
4	OutOfScope	0	0.00	
5	InScope	6	100.00	
6	Pass	3	50.00	
7	Missed	2	33.33	
8	False	1	16.67	
9	**SUMMARY**			
10	InScope	6	100.00	
11	Pass	3	50.00	
12	Missed	2	33.33	
13	False	1	16.67	
14	Pass+False+Missed	6	100.00	
15				
16				

Figure 5.9: Excel report example 2 - Statistics.

6

Discussion

The performance of the suggested brake light detection algorithm is discussed in this chapter, together with its main limitations and reasons for false and missed events. Rear lights with LED lamps are described together with illustrating images of how these lights are perceived by the camera and how they influences the performance of the brake light detection. The brake light detection algorithm was also tested in daylight, something that wasn't intended from the beginning and this is presented in the final section of this chapter.

Brake lights have very different shapes, brightnesses and they are also found in various positions on vehicles depending on the car model. Larger vehicles like trucks and buses usually have several small brake lights but no center high mounted stop lamp, which makes brake light detection more difficult. The difference in brightness for when the brake lights are lit can also be less than for smaller vehicles. At close range it might be possible to observe lit brake lights on such large vehicles but at longer range (maybe above 30 meters) it is hard to see the difference even for the naked eye. But even if we only focus our attention to vehicles equipped with a center high mounted stop lamp, detecting brake lights will be a complex task and you need to be able to handle all kinds of different situations in order for the algorithm to make the right decisions.

The brake light detection algorithm encountered many situations and most of them were handled in a correct way as Table 5.3 has shown. The brake light detection algorithm has a false detection rate of about 15% and misses about 1% of all brake light events. Both the *sensitivity* and the *specificity* are well above 90%, meaning that the brake light detection algorithm is good at detecting true brake lights and not detecting false events. It is possible to decrease the number of false detections by more narrow tolerance levels for the bright spot matching, but for verification purposes, it is more important to detect all true positives than to minimize the false positives.

It is often possible to only use the classifier (QDA) for brake light detection of vehicles ***in the same lane***, i.e. the two confirmation methods can be excluded in such case.

The reason is that the tolerance levels can be lowered for vehicles in path, due to less skew perspective of the brake lights.
The conclusions drawn from the performance of the two classification methods is that both LDA and QDA perform well. The LDA (often) makes a correct classification as long as the vision algorithm is successful in its analysis, thus finds all the associated brake lights. The QDA on the other hand is more robust in its classification, it is less dependent on the vision algorithm to give a correct output. This is exemplified with the failed sample (see Figure 5.1) in section 5.1 where the vision algorithm only manage to differentiate two of the three rear lights and yet the QDA makes the right classification (see Figure 5.4). Bottom-line is that QDA is more robust and manages to classify brake lights without CHMSL as long as the other brake lights are large enough.
The main limitation of the proposed brake light detection algorithm is that $\Delta\mu$ needs several frames to evaluate the brake light detection and therefor really short brake lights events, let's say less than 0.5 seconds, might be perceived as noise, thus ignored and missed.
Only for clarification, the red markers in the images and the brake light indicator in the bottom left corner of the right image in the following figures are only based on the first classification stage based on what the classifier (the instantaneous classification) suggests, hence it is not the final classification. In the same way are the blue markers indicating that no brake lights are present.

6.1 False events

The false detections were often due to interference of oncoming vehicles' headlights, especially when one of the headlights was observed right above the vehicle in front, hence mimics a center high mounted stop lamp. In most cases these false detections are filtered out by the classification confirmation methods described in section 4.5.2. However, 15% of the detected brake light events were false and the main reason is external light sources perceived as a CHMSL. The problem scenarios in city- and motorway traffic are presented here below.
City traffic often means lower speed limits, short distances to other vehicles or road users and there are also more stationary light sources (street lamps, shop windows, and advertisements) compared to rural roads. Stationary light sources like street lamps are not a big problem as long as the ego-vehicle (and subject-vehicle) are not traveling at low speed (below 30 kph), because then those lights only appear for a short period and can be filtered out as noise. In city traffic, the speed is limited to 50 kph and queues are common. This makes it possible for external light sources such as street lamps to interfere with the rear lights of vehicles for several consecutive frames. In cases like this the external light sources can be perceived as brake lights (CHMSL), which causes false detections. Figures 6.1 to 6.3 are some examples of city traffic situations. Figures 6.1 and 6.2 show how an external light source (street lamp in this case) is found within an object's bounding box, centered between the two side rear lights and therefor it is perceived as a center high mounted stop lamp.

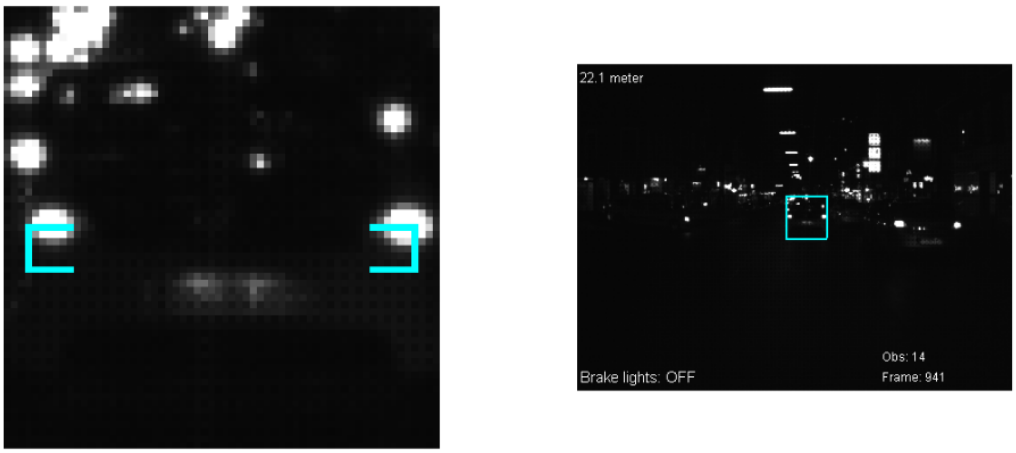

Figure 6.1: City traffic example 1.

Figure 6.2 shows how a street lamp can be mistaken as a CHMSL, which leads to a misclassification of the classifier.

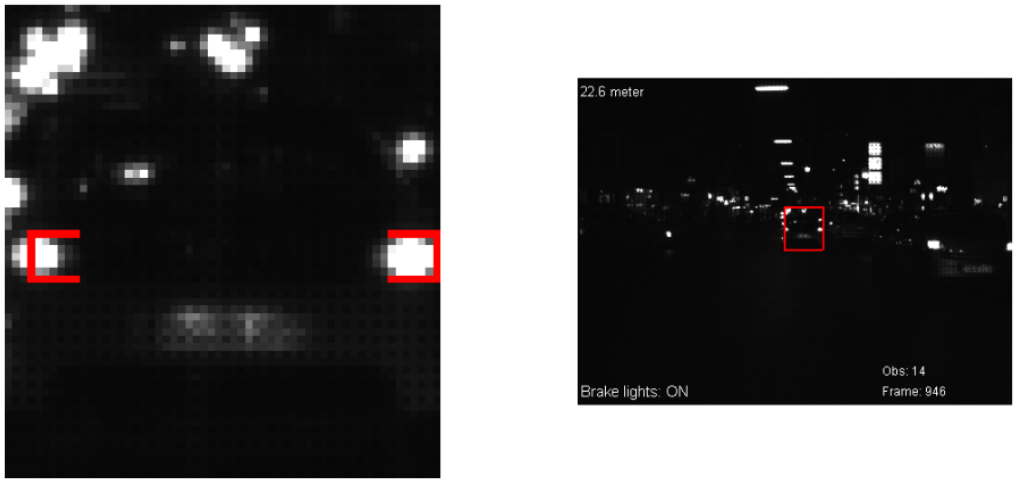

Figure 6.2: City traffic example 2 - false brake light detection.

Figure 6.3 shows a braking vehicle in city traffic.

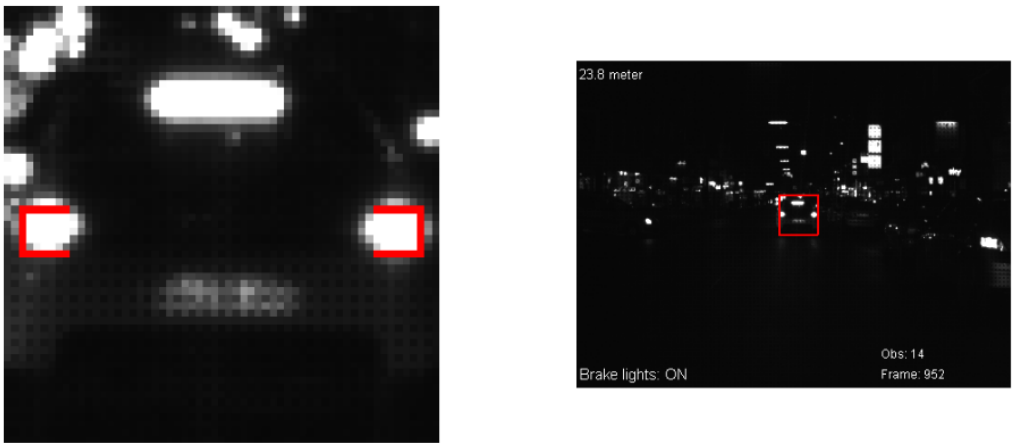

Figure 6.3: City traffic example 3 - true brake light detection

On motorways, vehicles often travel at high speed so as was mentioned before, stationary light sources are less likely to interfere with the vehicles' rear lights causing false brake light detections. Figures 6.4 to 6.6 illustrate another problem situation, namely oncoming traffic and interfering headlamps. One single oncoming vehicle is rarely causing problems like this unless it is far away and the motorway curvature makes it possible to observe the oncoming vehicles headlamps within the bounding box of the vehicle ahead for a longer period of time. Multiple oncoming vehicles on the other hand, as can be seen in the images in Figure 6.5, is a bigger issue. These headlamps tend to merge together and form a bright line, something that can easily be mistaken for a center high mounted stop lamp. In worst case, this bright line of merged headlamps appears in the top view of a vehicle's bounding box, the classifier will classify them as brake lights. The average-comparison method ($\Delta\mu$) would not be able to disregard the falsely detected brake lights since the false CHMSL will be observed for several consecutive frames. The only way to discover such false events is to look at ΔA_{side}, and as long as the side rear lights do not increase in size the false brake light detection will be reclassified and ignored. However, LED lamps or noise in terms of visual obstruction or interfering light sources can lead to size differences for the side rear lights between frames and in such case it would lead to false detections of brake lights.
Figure 6.4 shows a false classification of brake lights due to interfering headlamps seen through the windows of the subject vehicle.

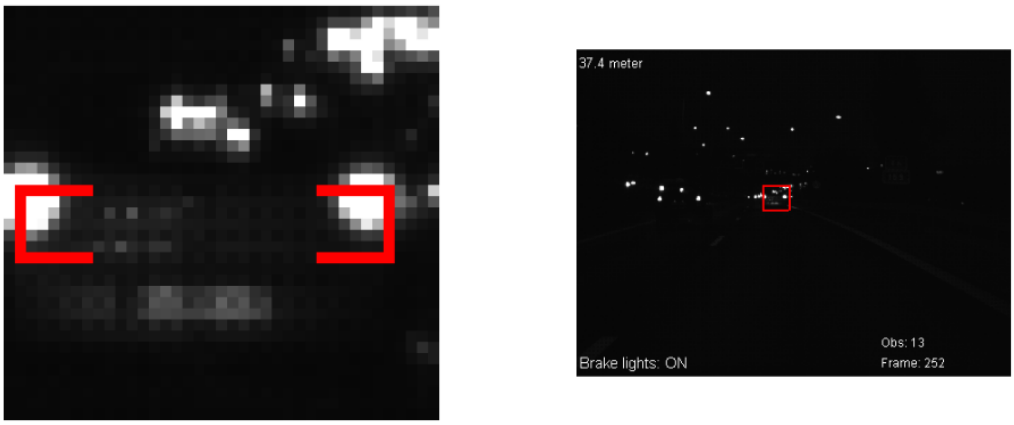

Figure 6.4: Motorway traffic example 1 - false brake light detection.

The images in Figure 6.5 show how the headlamps of multiple oncoming vehicle can cause false brake light detections.

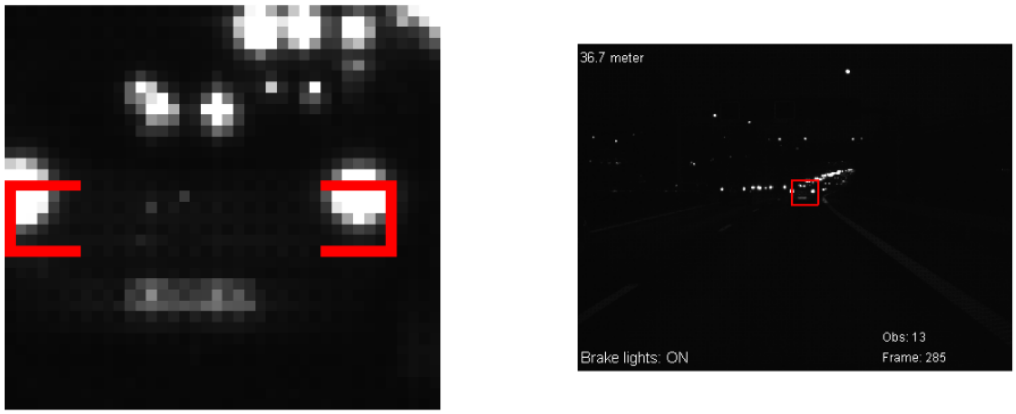

Figure 6.5: Motorway traffic example 2 - false brake light detection.

Figure 6.6 shows another false classification of brake lights due to interfering headlamps visible above the roof of the subject vehicle. In a gray-scale single frame image like this, it is really hard to see the difference with the naked eye.

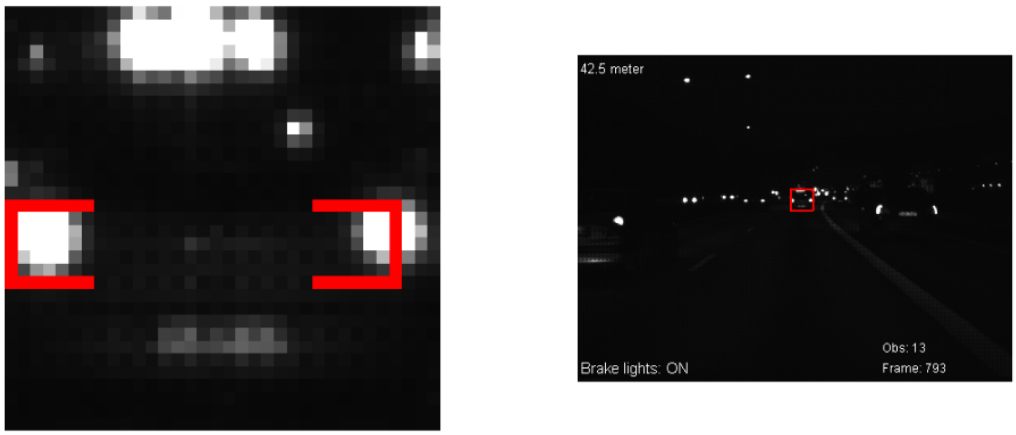

Figure 6.6: Motorway traffic example 3 - false brake light detection.

6.2 Missed events

Missed events can be caused by visual obstruction and in such case it is not much you can do about it. The brake light detection algorithm presented in this report missed four brake light events and one of the four missed brake light events was because the bounding box wasn't large enough to enclose the entire vehicle (a large transport van), exactly like the left image in Figure 4.14 illustrates but this time not even the Kalman updated bounding box was tall enough to cover the CHMSL. Brake lights on pickup trucks might also be difficult to detect since their CHMSL is often located on the cabin in front of the loading platform. This can cause a skew perspective of the brake lights, especially if the CHMSL is relatively small compared to the side brake lights, which then can be perceived as noise (i.e. small light source seen through the window). Another problem scenario is turning vehicles, either the ego or the subject vehicle. Such situations are short, often less than 10 image frames which is a problem itself because a short brake light event might be perceived as a false event due to temporary interfering of external light sources. Longer brake light events are therefor more easy to evaluate. In addition to that, a turning vehicle introduces an oblique perspective of the brake lights (the visual appearance, relative positions and offsets of the brake lights become distorted), which with the current tolerance limits of the spot matching will lead to no matched rear light pairs or discarded CHMSL. There is however a possibility to introduce a projective transform for correction of perspective distortion, presented in paper [6], that might solve this problem.

6.3 LED lights

The main difference between LED lights and non-LED lights is that LED lights are pulsed during non-braking situations, hence the lights blink with a certain frequency. The blinking LED rear lights can be observed in two consecutive frames shown in Figures 6.7

and 6.8. The blinking of rear lights with LED lamps is not perceived by the human eye. LED brake lights are however either constantly lit or pulsed with a higher frequency, so LED lights are not a problem per se. Although it will make it more difficult to catch false brake light detections because it has an oscillating effect on ΔA_{side}. If the oscillations in ΔA_{side} exceeds $T_{\Delta A_{side}}$, then ΔA_{side} becomes useless for brake light confirmation.

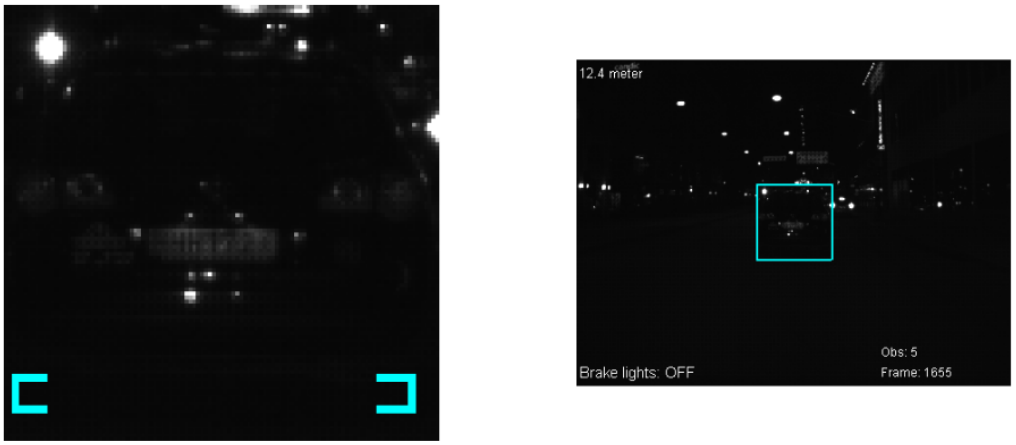

Figure 6.7: LED lights example 1.

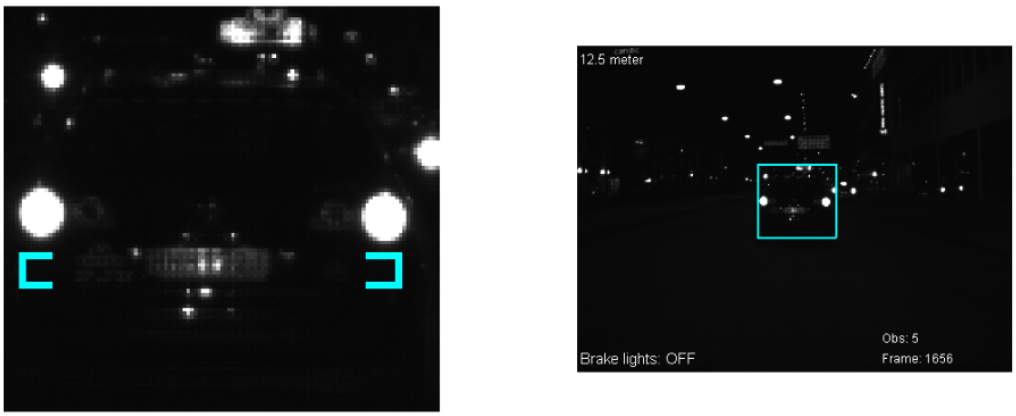

Figure 6.8: LED lights example 2.

Figure 6.9 shows brake lights with LED lamps.

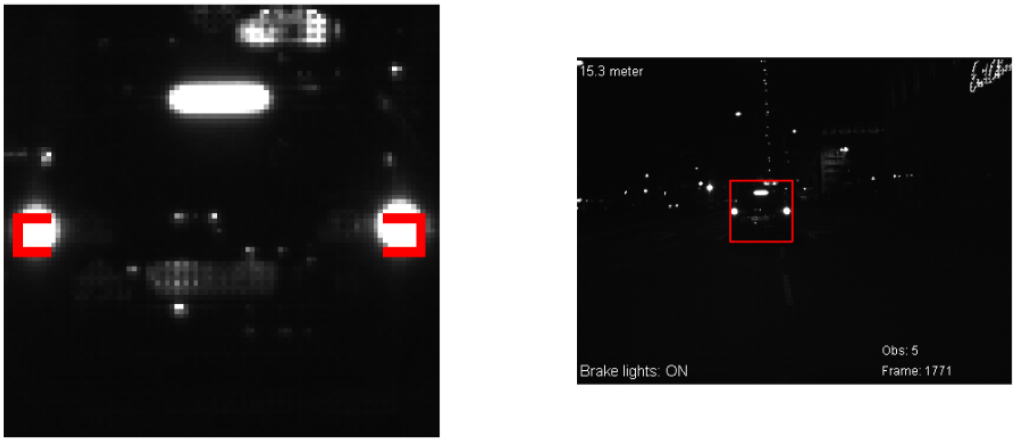

Figure 6.9: LED lights example 3 - true brake light detection.

6.4 Brake light detection in daylight

The brake light detection algorithm was tested in daylight. Five logged videos were analyzed and the brake light detection algorithm showed a success rate of 100%. The great result can be explained by the limited data set. The images in Figures 6.10 and 6.11 show that the brake lights are correctly detected. The conditions for detecting brake lights in daylight is different from brake light detection in dark conditions. The intensities for bright spots associated with rear lights are still saturated. There are less interference from external light sources such as street lamps but bright sunlight together with less bright brake lights will make it difficult for the vision algorithm to distinguish or even to find the appropriate candidate spots. However, the light conditions in this limited data set made it possible for the vision algorithm to easily find the right candidate spots, which lead to a correct decision-making in the brake light detection.

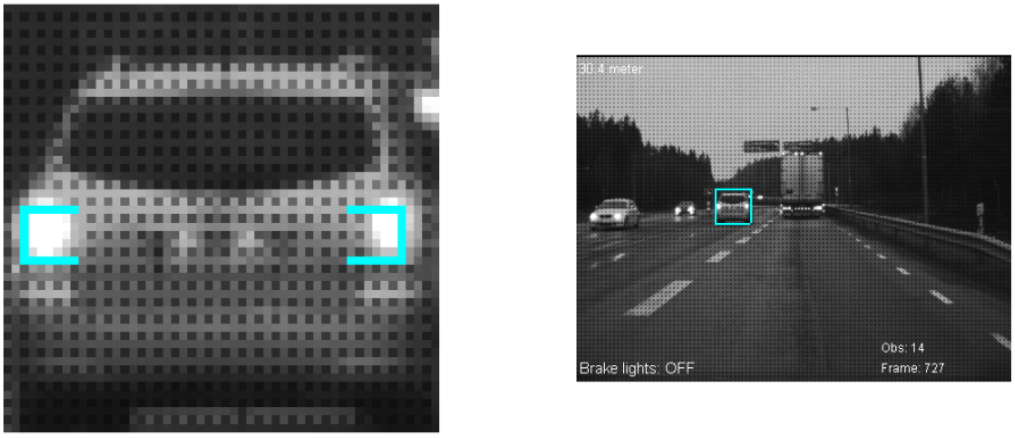

Figure 6.10: Brake light detection in daylight - no brake lights.

The images in Figure 6.11 show brake lights detected in daytime.

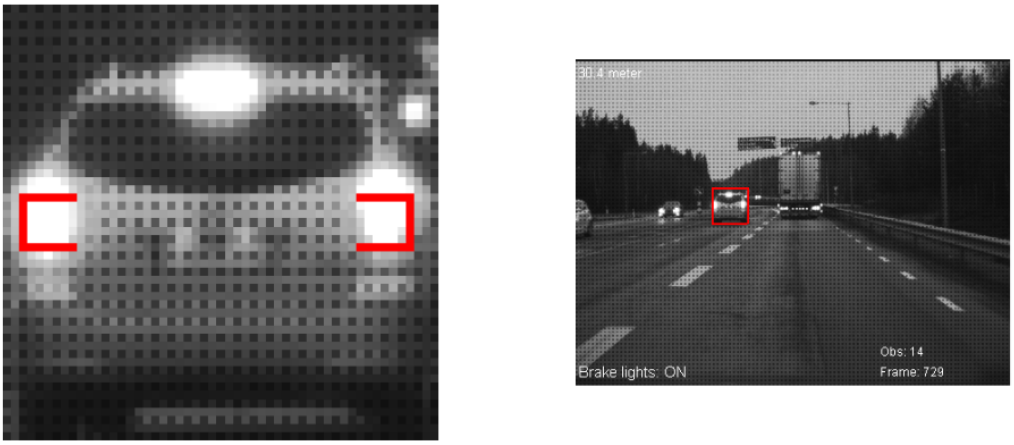

Figure 6.11: Brake light detection in daylight - brake lights detected.

7

Conclusion

The results have shown that the suggested brake light detection algorithm is able to detect brake lights on other vehicles in adjacent lanes regardless of the color of the light, the speed and the range. It also seems to be applicable on brake lights in light conditions. Vision-based brake light detection in gray-scale image frames is a complex task because any kind of light can be mistaken for a brake light since you don't know its true color.
Alone, neither of the three methods (QDA, $\Delta\mu$ and ΔA_{side}) is robust or reliable enough to provide a good result, but all together they complement each other and form a more robust and reliable method for brake light detection with a built-in correction of misclassifications.
The purpose of this thesis project was to improve the performance and efficiency of active safety system sensor verification. The brake light detection algorithm finds brake light events automatically and doesn't need any supervision when it processes the video data. It took about 190 minutes for the algorithm to process about 927 minutes of logged video data and to detect 432 brake light events (367 true and 65 false). All these events, together with the events found by the sensor system itself were then evaluated in the support tool (shown in Figure 5.7). A rough estimation would be that about 5-8 events can be evaluated in the support tool per minute. The evaluation process is fast because you will quickly notice if the sensor output is correct of not.
To manually watch all the video data would take almost 16 hours and in addition to that, lets say that the manual evaluation of the sensor system's brake light detection would take about 4 hours (probably more), then we end up with about 20 hours of manual work.
The support tool makes it possible to do the same job in less than 3 hours (based on 800 events and a process time of 5 events/min), which corresponds to about 12.5% of the time it would take to do the job manually.

7.1 Future work

Improvements to the brake light detection algorithm can be done in terms of bounding box optimization and extraction of red bright spots. A misaligned bounding box can lead to missed brake lights if the brake light detection algorithm only processes the sub-image within the bounding box. The Kalman based adjustment of the bounding boxes was successful in most cases but an optimization of the bounding box, i.e. a bounding box that surrounds the entire subject vehicle without to much additional space, could improve the performance and lower the false detection rate and the number of missed events. In addition to that, red light spots can be extracted by the use of so called red-clear filters and additional image pre-processing. In such case most of the false detections would probably be gone, since they often were caused by white light (headlamps or street light).
Suggestions for future work or further development, not necessarily for verification purposes, can be additional functions such as TTC (Time-To-Collision) estimation based on the relative distance between the rear lights, turning indicator detection, vehicle detection and of course also further development of brake light detection at daytime.

Bibliography

[1] M.-Y. Chern and P.-C. Hou, "The lane recognition and vehicle detection at night for a camera-assisted car on highway," *International Conference on Robotics and Automation*, 2003.

[2] W. Lui, C. Song, X. Wen, H. Yuan, and H. Zhao, "A monocular-vision rear vehicle detection algorithm," *Vehicular Electronics and Safety*, 2007.

[3] P. Thammakaroon and P. Tangamchit, "Predictive brake warning at night using taillight characteristic," *IEEE International Symposium on Industrial Electronics*, 2009.

[4] S. Görmer, D. Müller, S. Hold, M. Meuter, and A. Kummert, "Vehicle recognition and ttc estimation at night based on spotlight pairing," *Proceedings of the 12th International IEEE Conference on Intelligent Transportation Systems*, 2009.

[5] R. O'Malley, M. Glavin, and E. Jones, "Rear-lamp vehicle detection and tracking in low-exposure color video for night conditions," *IEEE Transactions on Intelligent Transportation Systems*, vol. 11, no. 2, June 2010.

[6] R. O'Malley, M. Glavin, and E. Jones, "Vision-based detection and tracking of vehicles to the rear with perspective correction in low-light conditions," *IET Intelligent Transport Systems*, 2010.

[7] M. Boumediene, A. Ouamri, and M. Keche, "Vehicle detection algorithm based on horizontal/vertical edges," *7th International Workshop on Systems, Signal Processing and Their Applications*, 2011.

[8] J. Tantalo, "Brake light detection by image segmentation," Department of Electrical Engineering and Computer Science, CASE University, Cleveland, Ohio, Tech. Rep., 2006.

[9] A. Fossati, P. Schönmann, and P. Fua, "Real-time vehicle tracking for driving assistance," *Machine Vision and Applications*, vol. 22, pp. 439–448, 2011,

10.1007/s00138-009-0243-6. [Online]. Available: http://dx.doi.org/10.1007/s00138-009-0243-6

[10] M. Rudemo, *Image analysis and spatial statistics*, 2009.

[11] D.-Y. Chen and Y.-H. Lin, "Frequency-tuned nighttime brake-light detection," Department of Electrical Engineering, Yuan-Ze University, Taiwan, Tech. Rep., 2010.

[12] C. J. Kahane and E. Hertz, "The long-term effectiveness of center high mounted stop lamps in passenger cars and light trucks," NHTSA, Tech. Rep., 1998.

[13] M. Sonka, V. Hlavac, and R. Boyle, *Image Processing, Analysis, and Machine Vision*, third edition ed. Cengage Learning, 2008.

[14] N. Funk, "A study of the kalman filter applied to visual tracking," University of Alberta, Tech. Rep., 2003.

[15] T. McKelvin, "A brief introduction to kalman filtering," Department of Signals and Systems, Chalmers University of Technology, Tech. Rep., 2011.

[16] T. Hastie, R. Tibshirani, and J. Friedman, *The Elements of Statistical Learning - Data Mining, Inference, and Prediction.* Springer-Verlag New York Inc., 2009.

[17] Biyee.net. (2011, March) Binomial confidence interval and its application in reliability tests. [Online]. Available: http://www.biyee.net/data-solution/resources/binomial-confidence-interval.aspx

[18] P. Mayfield. (2011, December) Understanding binomial confidence intervals. [Online]. Available: http://www.sigmazone.com/binomial_confidence_interval.htm

[19] J. Sauro. (2005, October) Confidence interval calculator for a completion rate. [Online]. Available: http://www.measuringusability.com/wald.htm

[20] A. Boomsma, "Confidence interval for a binomial proportion," Department of Statistics and Measurement Theory, University of Groningen, Tech. Rep., 2005.

[21] Statsoft.com. (2012, March) Distribution tables. [Online]. Available: http://www.statsoft.com/textbook/distribution-tables/#f05

A

Appendix

A.1 Vision algorithm reliability test

The success rate of the vision algorithm is a measure of how reliable the algorithm is on detecting the correct spots associated with rear lights. One method could be to use MLE (Maximum Likelihood Estimation), which is the number of successful trials (X) divided by the total number of trials (N). However, if the size of the sample set is small and the number of failed trails are few or none the accuracy of such a method tends to be low (example: $N = 30$ and $X = 30$ gives a success rate of 100%). A more accurate method in such a case is the *Exact method* also called the *Clopper-Pearson interval*, which is a one-sided binomial confidence interval and since it is a reliability test only the lower bound is concerned and the confidence level is set to 95% (the same example again using the *Exact method* gives a success rate of 90% with a confidence level of 95%) [17–19].

The lower bound of the confidence interval can, according to [20], be defined as:

$$CI_{low} = \frac{X}{X + (N - X + 1)F} \tag{A.1}$$

Here F is 2.3719 for both sets (the F-quantile obtained from the F-distribution table using $\alpha = 0.05$, column = 2 (N-X+1) and row = 2X) [21].

A.2 Decision boundaries

A.2.1 LDA

The decision boundary of an LDA is a straight line (equation A.2).

$$y = k \cdot x + m \tag{A.2}$$

Here k and m can be extracted from equation 4.21 and expressed as A.4 and A.5:

$$\boldsymbol{C} = \begin{bmatrix} C_{11} & C_{12} \\ C_{21} & C_{22} \end{bmatrix} \tag{A.3}$$

$$k = \frac{(C_{11}^{-1}\mu_1 - C_{12}^{-1}\mu_2)}{(C_{21}^{-1}\mu_1 - C_{22}^{-1}\mu_2)} \tag{A.4}$$

$$m = -\frac{(\mu_1 + \mu_2)\boldsymbol{C}^{-1}(\mu_1 - \mu_2)}{2(C_{21}^{-1}\mu_1 - C_{22}^{-1}\mu_2)} \tag{A.5}$$

A.2.2 QDA

The decision boundary of a QDA is a quadratic function (equation A.6).

$$y = ax^2 + bx + c \tag{A.6}$$

The derivation of the constants in equation A.6, extacted from equation 4.22 are solved in the same way as for the LDA, but these expressions are long and less easy to present nicely in a report like this and will therefor be left out.

A.3 $\Delta\mu$ peak limit estimation

Here is the estimation of the $\Delta\mu$ threshold for different bounding box widths. 30 braking events were evaluated and the $\Delta\mu$ peak values are plotted against the width of the bounding box (see Figure A.1). The threshold is obtained by linear interpolation of these peak values.

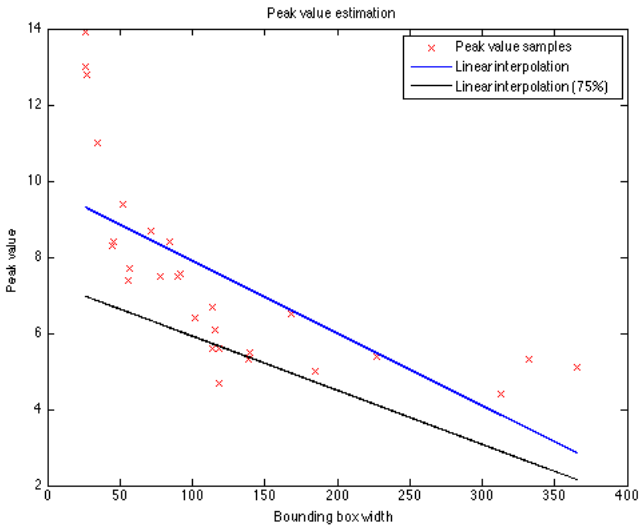

Figure A.1: Interpolation of peak values.